

# Hypothesis Test of the Photon Count Distribution for Dust Discrimination in Dynamic Light Scattering

David Bossert,<sup>□</sup> Federica Crippa,<sup>□</sup> Alke Petri-Fink,<sup>□,§</sup> and Sandor Balog<sup>□\*</sup>

<sup>□</sup> Adolphe Merkle Institute, University of Fribourg, Chemin des Verdiers 4, 1700 Fribourg, Switzerland

<sup>§</sup> Chemistry Department, University of Fribourg, Chemin du Musée 9, 1700 Fribourg, Switzerland

Corresponding Author: sandor.balog@unifr.ch

## *Supporting Information*

Contents

<b>Methods and Materials</b> .....	2
Dynamic light scattering.....	2
Transmission electron microscopy .....	2
Silica nanoparticles.....	2
Iron oxide nanoparticles .....	2
Gold nanoparticles.....	3
<b>Analysis and results</b> .....	3
Iron oxide nanoparticles .....	3
Gold nanoparticles.....	4
Field auto correlation functions and the corresponding photon count traces of the gold nanoparticles.....	6

## Methods and Materials

### Dynamic light scattering

Using 2 ml of a dilute aqueous suspension of the particles, data were collected at constant temperature (21 °C) on a commercial goniometer instrument (3D LS Spectrometer, LS Instruments AG, Switzerland). The primary beam was formed by a linearly polarized and collimated laser beam (Cobolt 05-01 diode pumped solid state laser,  $\lambda = 660$  nm,  $P_{max} = 500$  mW), and the scattered light was collected by single-mode optical fibers equipped with integrated collimation optics. The incoming laser beam passed through a Glan-Thompson polarizer with an extinction ratio of  $10^{-6}$ , and another Glan-Thompson polarizer, with an extinction ratio of  $10^{-8}$ , was mounted in front of the collection optics. To construct the intensity auto-correlation function  $g_2(t)$ , the collected light was coupled into two APD detectors via laser-line filters (Perkin Elmer, Single Photon Counting Module), and their outputs were fed into a two-channel multiple-tau correlator. To improve the signal-to-noise ratio and to eliminate the impact of detector after-pulsing on  $g_2(t)$  at early lag times below 1  $\mu$ s, these two channels were cross-correlated. The field auto-correlation function was obtained via the Siegert relation:  $g_1(t) = \sqrt{g_2(t) - 1}$ . Without any modification made, the photon counts of one of the APD detectors were obtained through the same detection line as above, at a sampling rate of  $\sim 9.5$  Hz ( $\tau = 0.105$  s integration time).

### Transmission electron microscopy

TEM micrographs of the NPs were taken with a Tecnai Spirit transmission electron microscope (FEI) at 120 kV. The images were recorded at a resolution of  $2048 \times 2048$  pixels (Veleta CCD camera, Olympus). 1  $\mu$ l of particle suspension was drop-cast onto a carbon-film square mesh copper grid (Electron Microscopy Sciences, CF-300-Cu), diluted on the grid with EtOH (5  $\mu$ l, 99.98%, VWR chemicals) and excess liquid was soaked with a tissue (KIMTECH, precision wipes). The grid dried under a modest flow of nitrogen. For particle characterization, the micrographs were bi-leveled in ImageJ (National Institutes of Health NIH, USA) using the default threshold method (IsoData-based variation).<sup>1</sup> The binary images were analyzed by a built-in routine (Analyze Particles) without separation methods and constrains.

### Silica nanoparticles

In a round-bottom flask with an attached reflux condenser, water (116 ml), ammonia (15.6 ml) and ethanol (EtOH, 324 ml) were heated to 70 °C and equilibrated. After 1 hour, tetraethoxysilane (TEOS, 32 ml) was added and the reaction mixture was stirred at 70 °C overnight. The mixture was then cooled to room temperature and washed by three centrifugation-dispersion cycles (EtOH, water, and water again). The silica nanoparticles (SiO<sub>2</sub> NPs) were further purified by dialysis against water for three days. The ammonium hydroxide (ammonia 25% solution, Honeywell), ethanol (HPLC-grade, Honeywell), and TEOS (99%, Merck) were used as received.

### Iron oxide nanoparticles

Superparamagnetic iron oxide nanoparticles (SPIONs) were synthesized by thermal decomposition of iron oleate-complex.<sup>2</sup> Briefly, 8.66 g of iron (III) chloride hexahydrate (FeCl<sub>3</sub>·6H<sub>2</sub>O, pur. 99 $\geq$ % Sigma-Aldrich) and 29.77 g of sodium oleate (pur. >97% TCI) were dissolved in a mixture of 64 ml ethanol, 48 ml distilled water and 112 ml hexane. The reaction mixture was heated to 70°C and kept at reflux for 4 hours under magnetic stirring. Afterwards the organic phase was washed 3

times with 50 ml distilled water in a separator funnel, the hexane was evaporated and the final iron oleate-complex was stored at 4°C. Oleic acid coated SPIONs have been synthesized as follows: 15.9 g of freshly prepared iron oleate-complex and 2.5 ml of oleic acid (pur. 90%, Aldrich) were dissolved in 115.3 ml of trioctylamine (pur. >97%, bpt:367°C, TCI) and degassed at 50°C for 2 hours. Then the solution was heated to 320°C under a constant flow of argon with a two-step heating process: first the temperature was quickly increased to 120°C (10 °C/min), and then the heating rate was decreased to 3°C/min and was kept constant until 320°C. The reaction was then maintained at this temperature for 60 minutes. After cooling, hexane and ethanol were added to precipitate the NPs and sequential centrifugations were performed to purify the SPIONs. To stabilize the SPIONs in water, surface grafted oleic acid was replaced with citric acid following a ligand exchange procedure.<sup>3</sup> Briefly, 110.6 mg of oleic acid coated NPs were re-dispersed in 30 ml of dichlorobenzene and dimethylformamide (ratio 1:1) and 92.16 mg of citric acid (pur. 99%, Sigma-Aldrich) were added. The dispersion was stirred and its temperature was maintained at 100°C for 24 hours. After, the NPs were precipitated in 100 ml of diethyl ether and recovered with a magnet. The particles were washed 3 times in acetone and finally re-dispersed in distilled water (milliQ).

#### Gold nanoparticles

Aqueous suspension of citrate-stabilized gold nanoparticles (Au NPs) were purchased and used as received (NIST standard reference material, RM 8011).<sup>4</sup> Prior to the measurements, the suspension was diluted six-fold into 2 mmol l<sup>-1</sup> NaCl solution, and passed through a 0.2 μm pore size PTFE membrane.

### Analysis and results

#### Iron oxide nanoparticles

Figure SI-1 shows the results on the SPIONs. At each scattering angle ( $\theta = 30^\circ, 31^\circ, \dots, 50^\circ$ ), fifty ten-second long correlation functions were collected. First, all the correlation functions were analyzed without testing whether or not the corresponding photon counts follow a normal distribution. Next, only the data that had passed the normality test was analyzed. For analysis, we used the method of cumulants, which is a model-free approach and essentially consists of fitting a low-order polynomial against the early data points of  $\ln g_1(t)$ . At moderate polydispersity values, usually a 2<sup>nd</sup>-order polynomial is used, and the linear term quantifies the scattering intensity-weighted relaxation rate ( $\Gamma$ ), where from the Z-average particle radius is determined directly via the Stokes-Einstein equation (Equation 2 and 3). Results show that the hypothesis test of normality on the photon count distribution has a strong impact on the quality of the characterization. Using the normality test prior to analysis results in precise numbers narrowly spread: the mean radius is  $R = 10.18$  nm, and the 95% confidence interval is 10.11-10.24 nm. Without test, these numbers are 23.23 nm, and 6.27-40.18, indicating a broad distribution of values. Even if we omit the outliers and set an arbitrary but plausible threshold at e.g. 20 nm, many values are above the ones obtained after the normality test. The radius as measured by TEM follows a narrow distribution with a mean of 9.2 nm (95% confidence interval for the population mean: 9.1-9.3 nm). The Z-average ( $\langle R^6 \rangle / \langle R^5 \rangle$ ) as estimated by TEM is 9.6 nm. The agreement between TEM and DLS is within 7%.

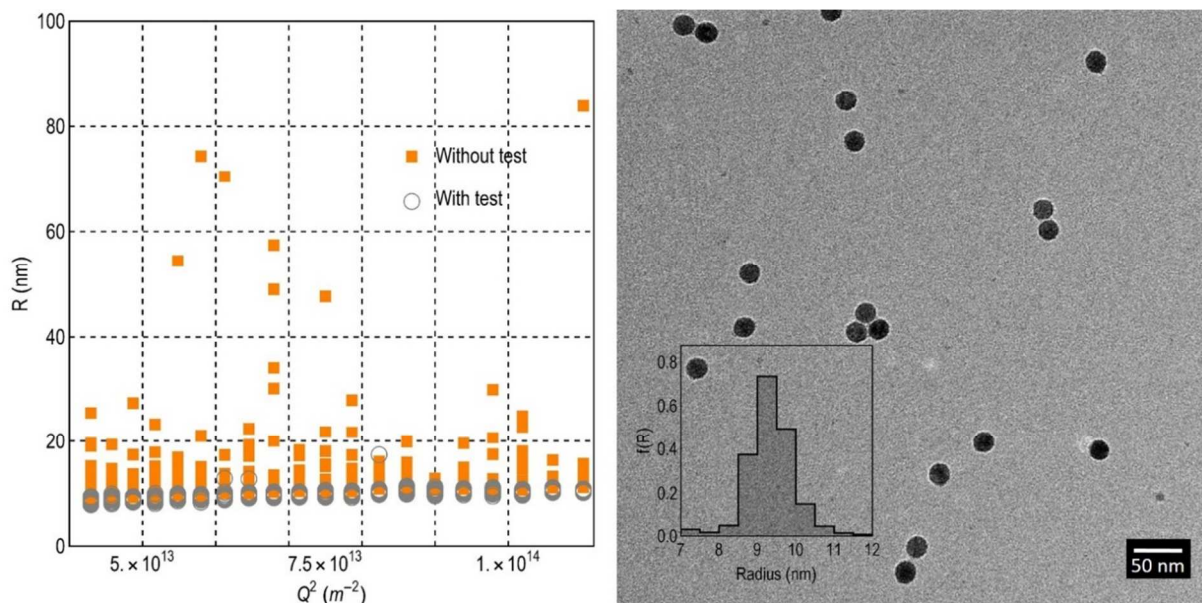


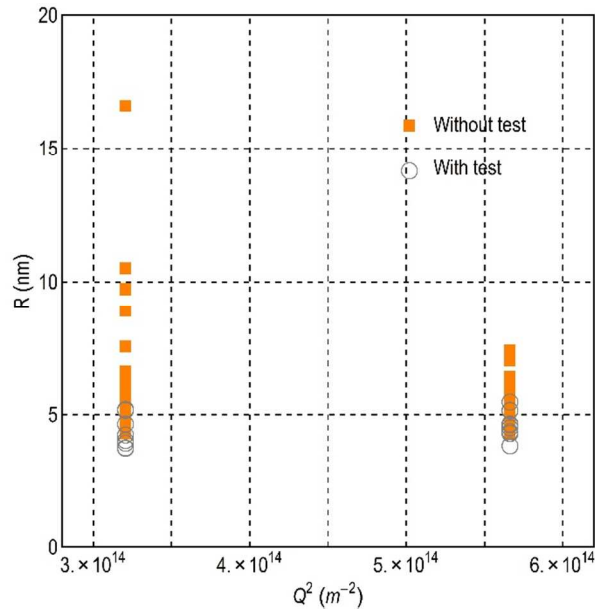
**Figure SI-1.** The analyses of SPIONs. Left: DLS analyses of the radii determined at different angles without and with normality test on the photon counts. At each  $Q$  value, photon count traces were collected with  $\tau = 0.525$  s integration time during 10 s. Right: TEM micrograph of the SPIONs and the result of the image analysis. Inset: The probability density function constructed by counting 583 particles.

#### Gold nanoparticles

These AuNPs are among the standard reference materials issued by NIST.<sup>4</sup> They are dedicated to "evaluate and qualify methodology and/or instrument performance related to the physical/dimensional characterization of nanoscale particles". Seven European national testing and metrology laboratories have measured these AuNPs.<sup>5,6</sup> Their study—reporting on fundamentally different techniques—atomic force microscopy, dynamic light scattering, small-angle X-ray scattering (SAXS), and electron microscopy—concluded that all methods, except DLS, provided consistent results. This inconsistency likely owes to the fact that the suspension is reported to contain a small percentage of clusters of primary particles beside the primary particles.<sup>4</sup> The primary particles, however, are expected to be monodisperse (coefficient of variation  $<2\%$ ) with a radius of 4.6 nm, as measured by SAXS.<sup>4,6</sup> NIST reports a Z-average radius of 6.8 nm, as measured by DLS in backscattering geometry ( $\theta = 173^\circ$ ) and using the method of cumulants. This result is still inconsistent both with their TEM (4.5 nm) and SAXS (4.6 nm) results.<sup>4</sup> This is despite the fact that 50% of the DLS measurements (the ones with the highest intensities) was removed as a dust rejection filter.

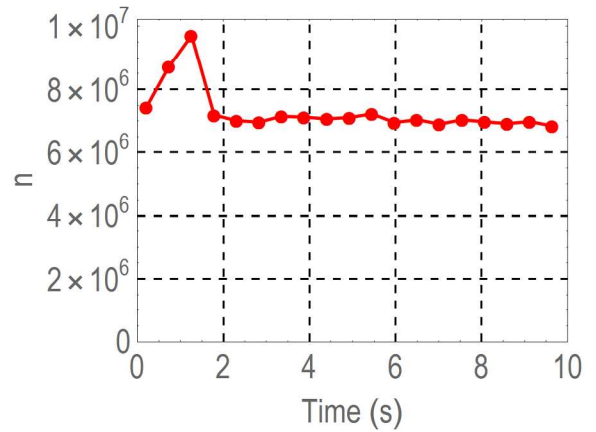
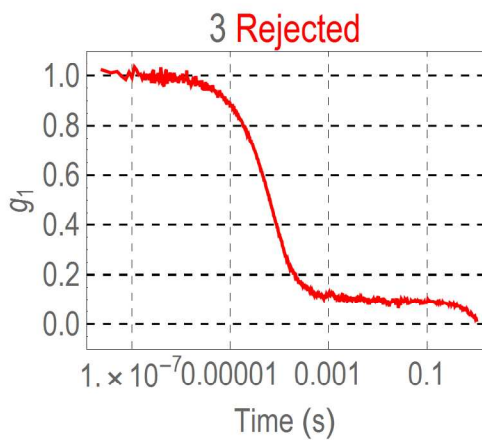
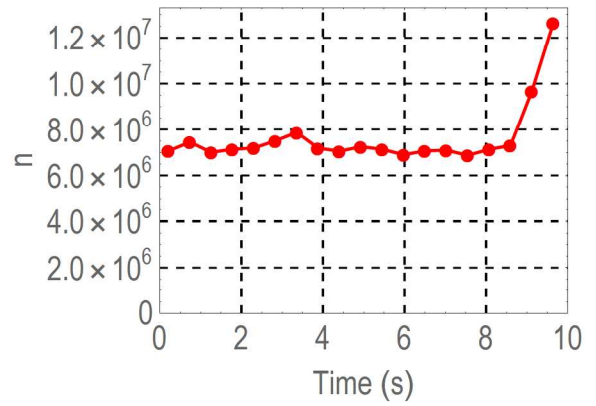
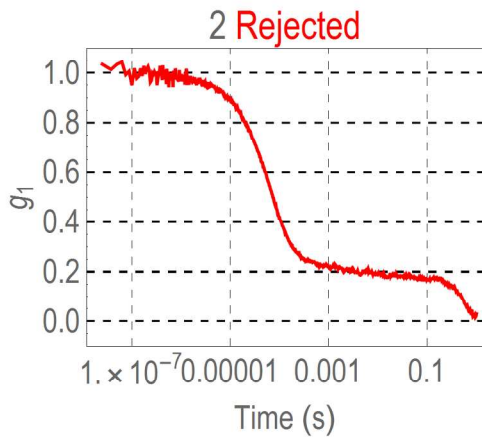
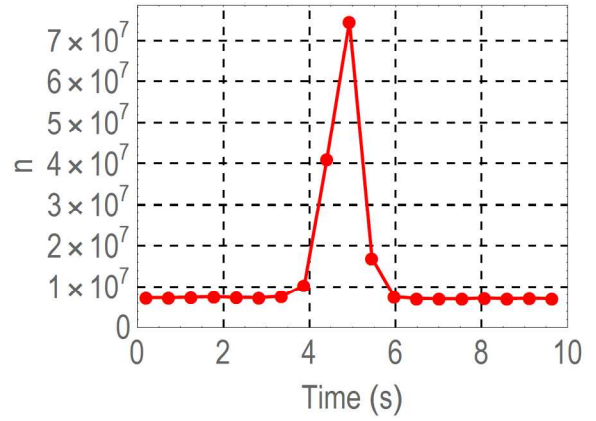
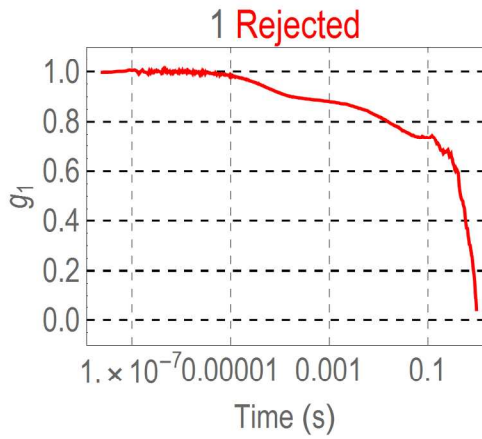
Figure SI-2 shows our DLS results on the AuNPs. In our case, data were recorded at two scattering angles ( $\theta = 90^\circ, 140^\circ$ ). First, all the correlation functions were analyzed by the method of cumulants without testing whether or not the corresponding photon counts follow a normal distribution. Next, only the data that had passed the normality test was analyzed. The normality test proves to be very effective as dust-rejection filter, and due to the presence of spikes and burst in the scattering intensity, only one-fifth of the measurements passed the normality test. The field auto correlation functions and the corresponding photon count traces of the citrate-stabilized gold nanoparticles are shown below, and the result of the normality test is indicated for each measurement. Next, we fitted a 2<sup>nd</sup>-order polynomial against the early data points of  $\ln g_1(t)$ , and determined the Z-average particle radius directly from the slope of the linear term. Results show that the

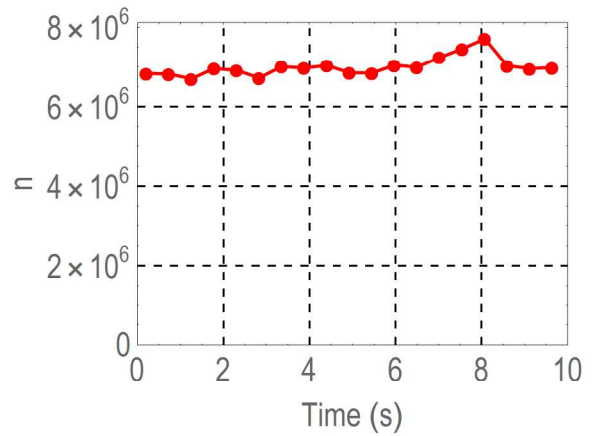
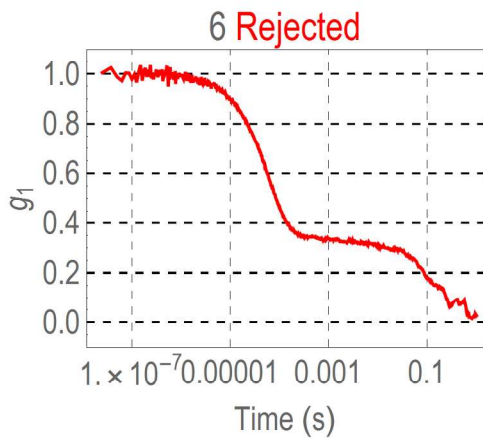
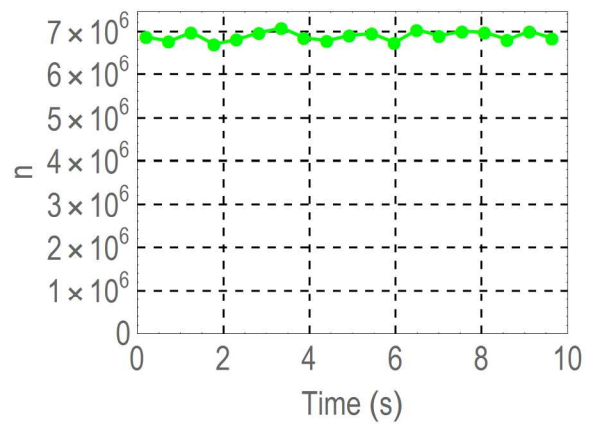
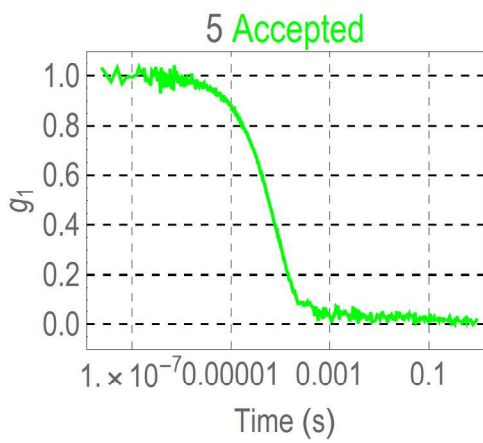
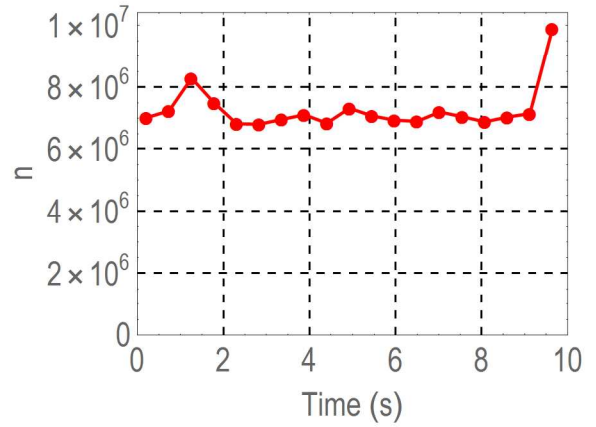
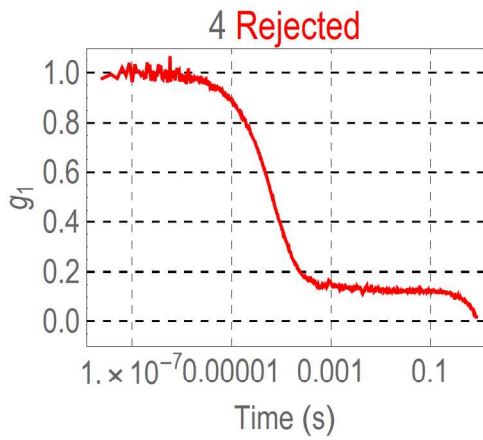
hypothesis test of normality on the photon count distribution has again very strong impact on the quality of the characterization. Using the normality test prior to analysis results in precise numbers narrowly spread: the mean radius is  $R = 4.6$  nm, and the 95% confidence interval is 4.3-4.8 nm. This is in nearly perfect agreement with the results obtained independently by others using SAXS and TEM. Without test, these numbers are 6.7 nm (NIST reports 6.8 nm), and 4.8-8.5 nm, due to the broader distribution of the measured values.

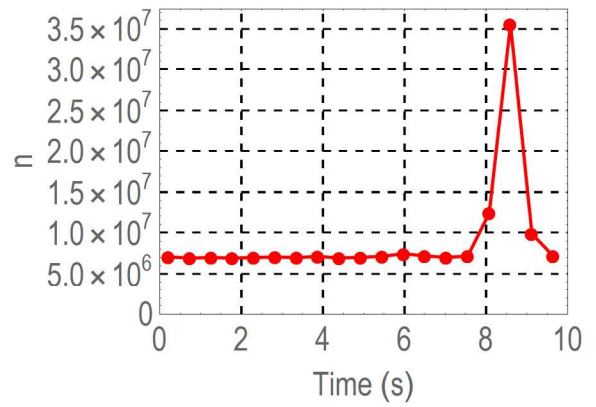
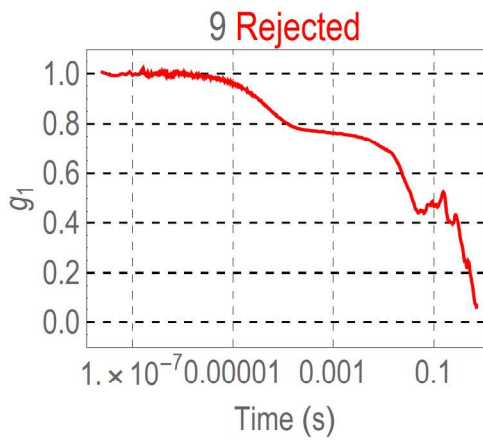
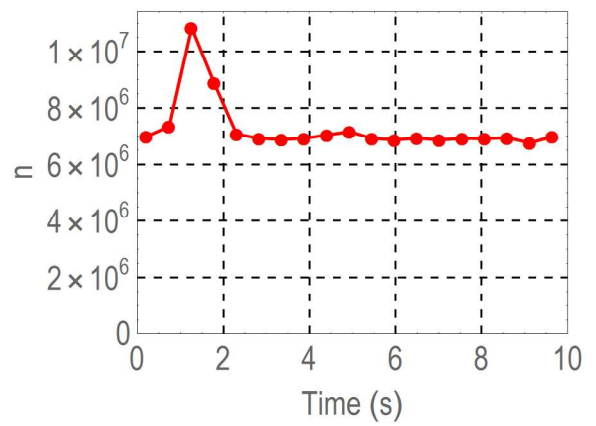
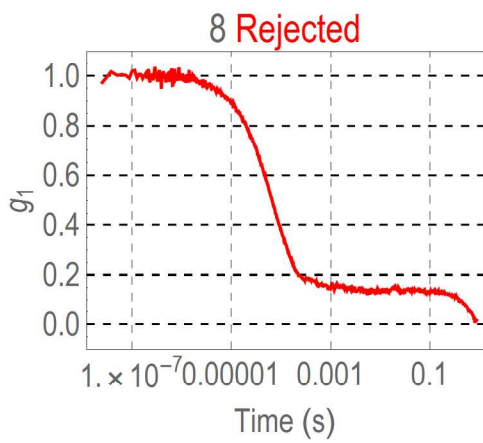
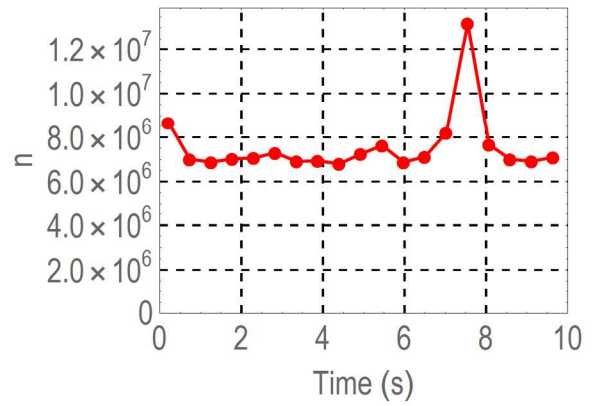
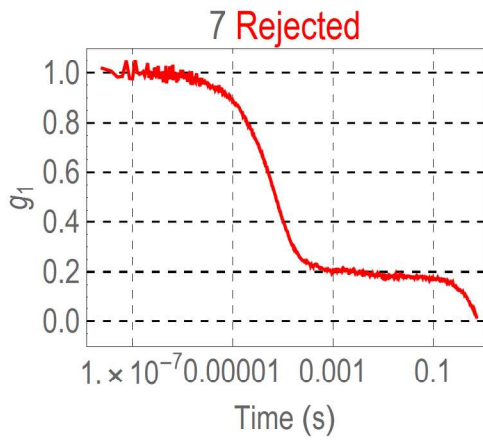


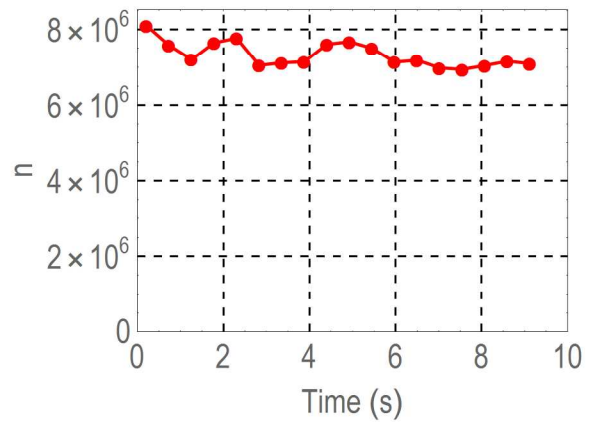
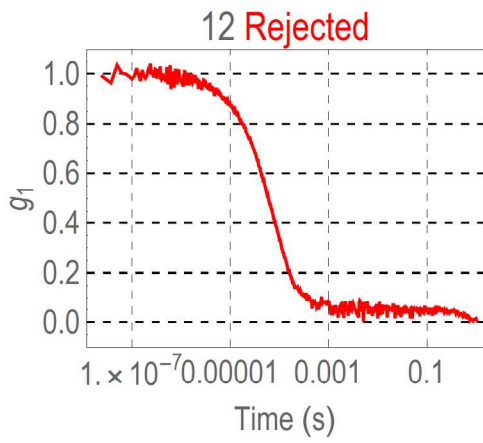
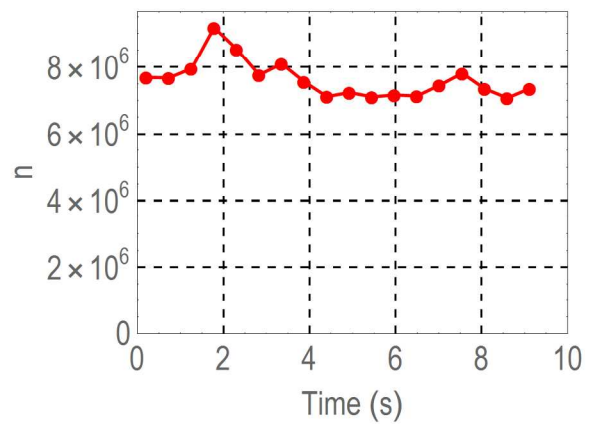
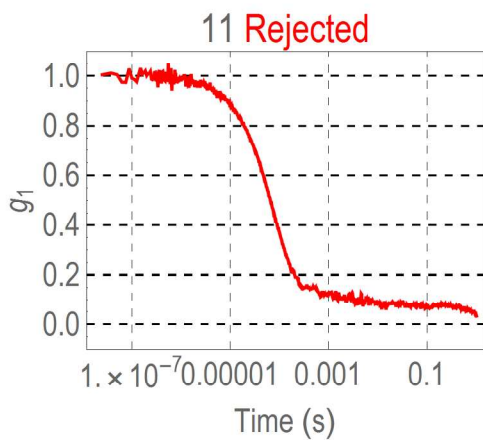
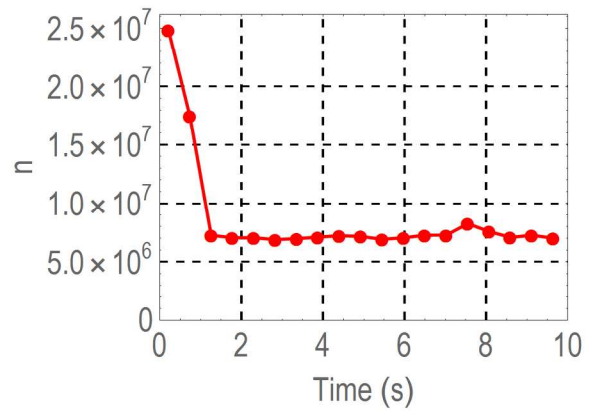
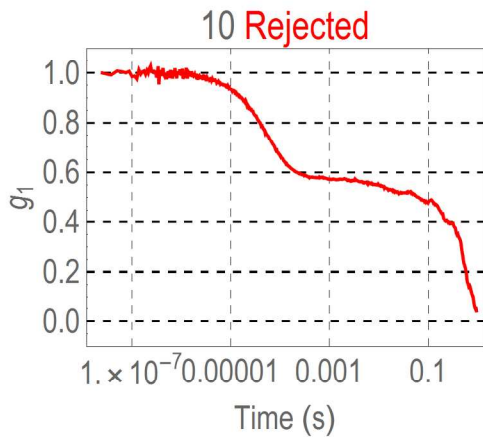
**Figure SI-2.** The DLS analyses of the AuNPs. The radii determined at two different angles without and with normality test on the photon counts. The photon count traces were collected with  $\tau = 0.525$  s integration time during 10 s.

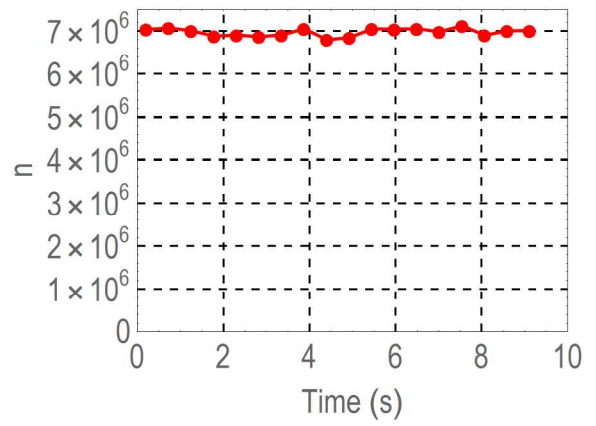
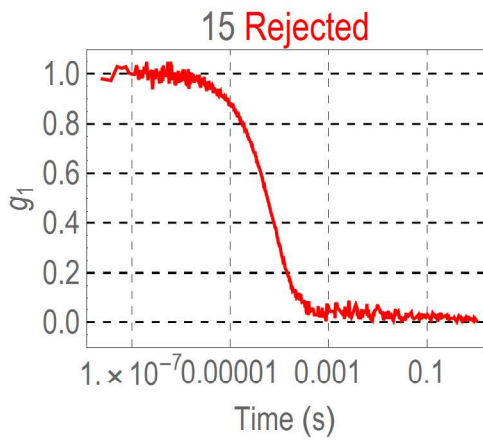
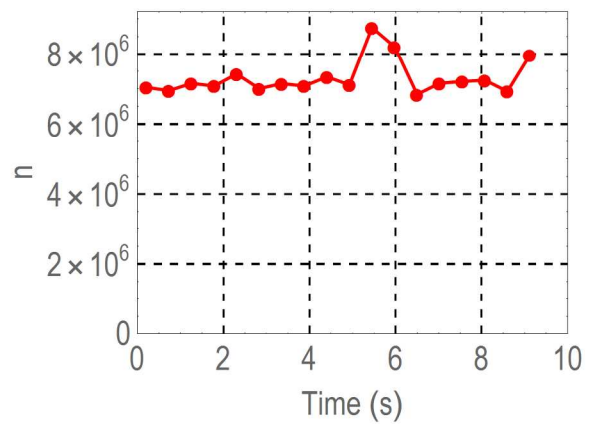
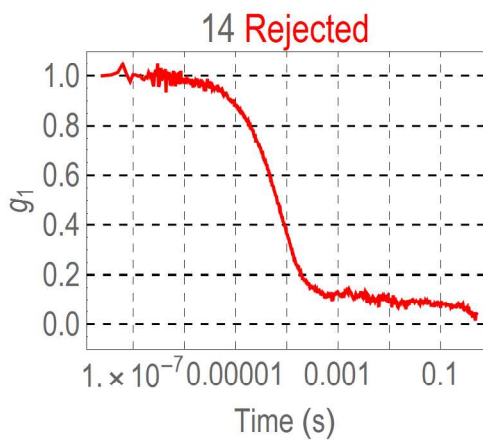
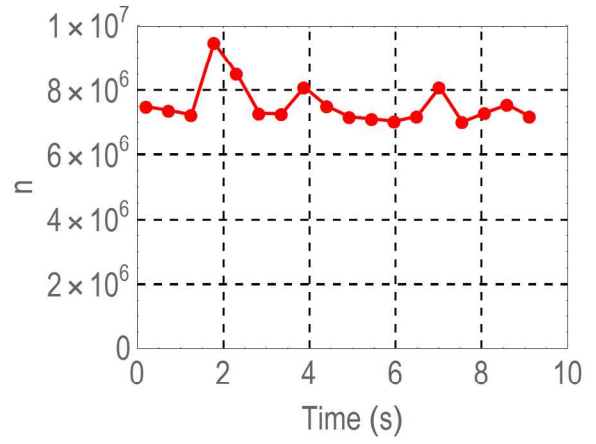
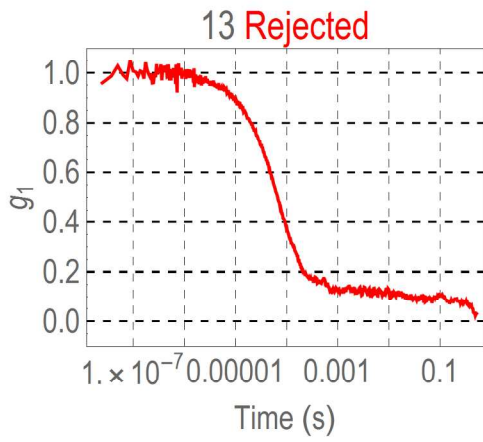
Field auto correlation functions and the corresponding photon count traces of the gold nanoparticles

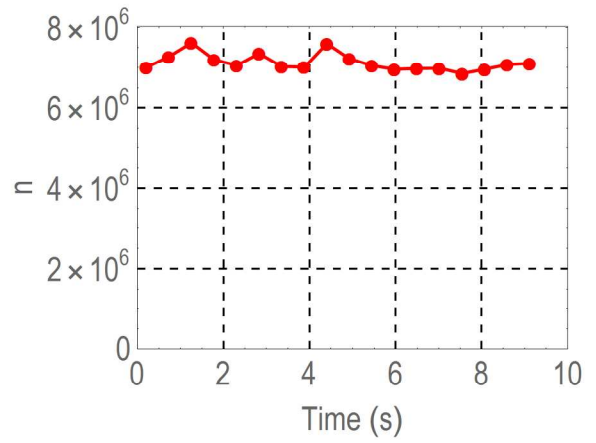
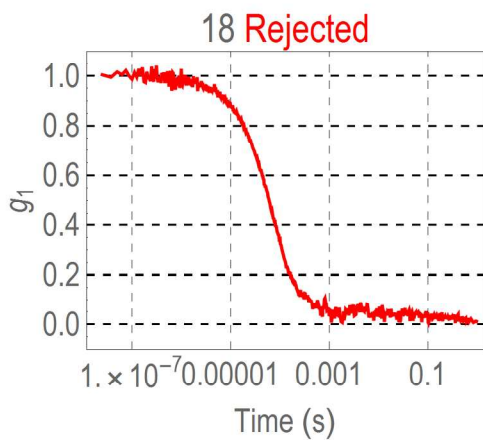
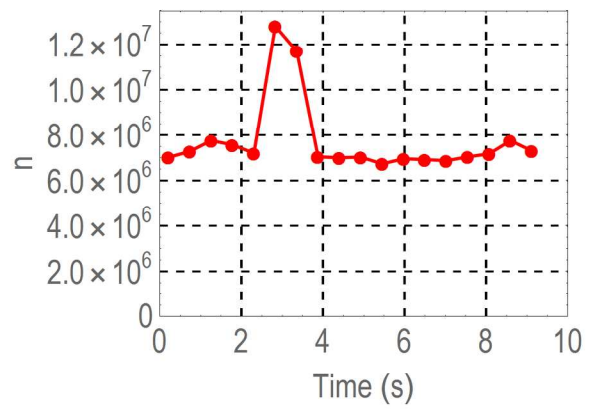
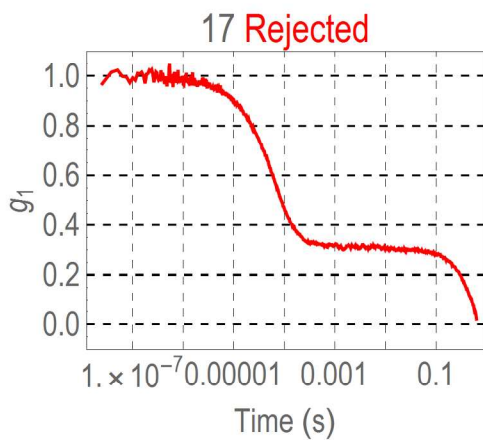
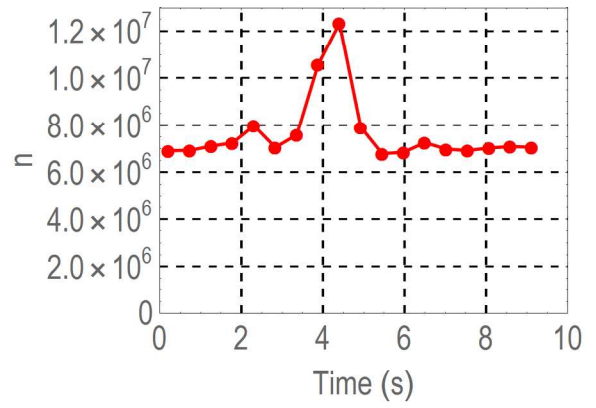
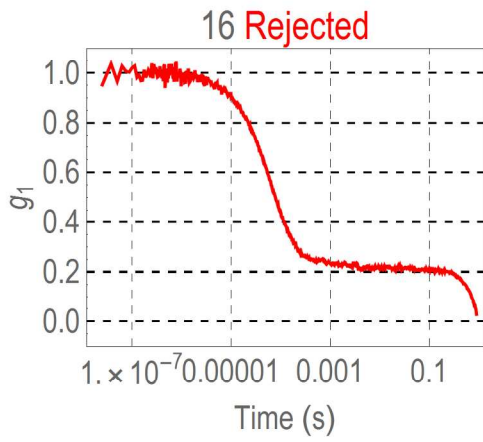


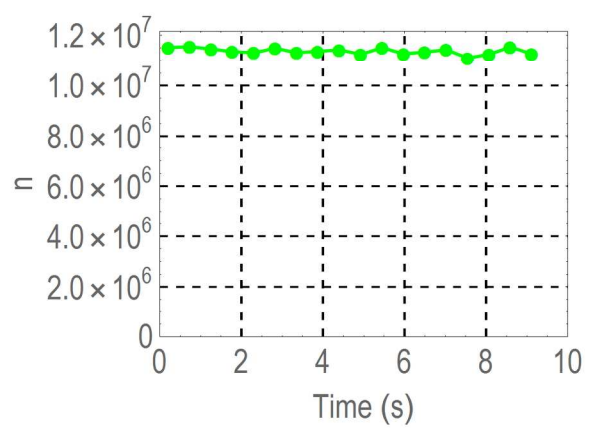
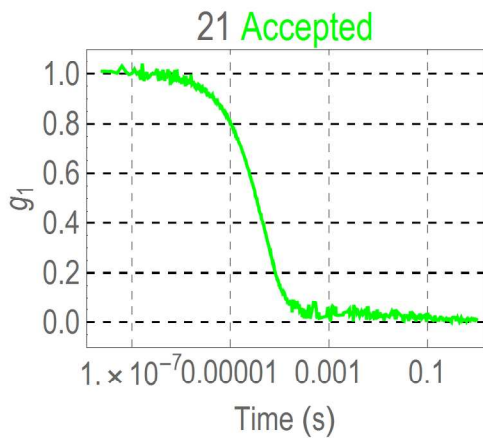
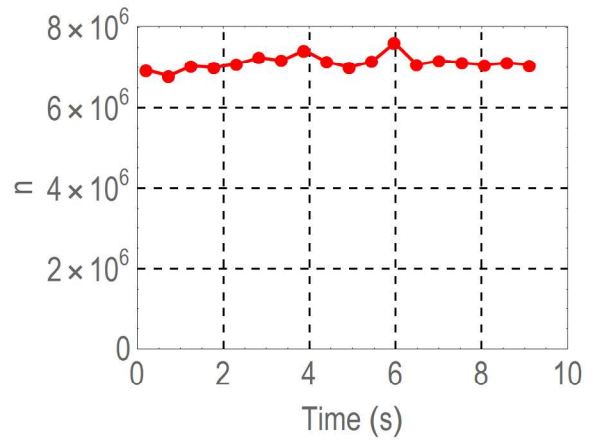
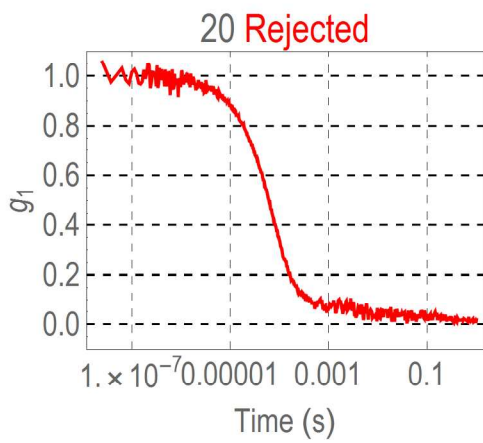
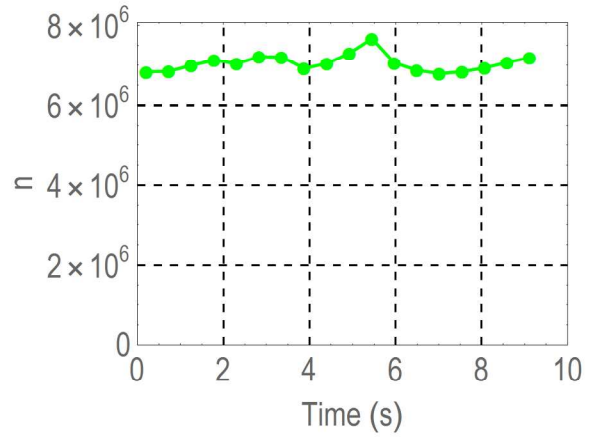
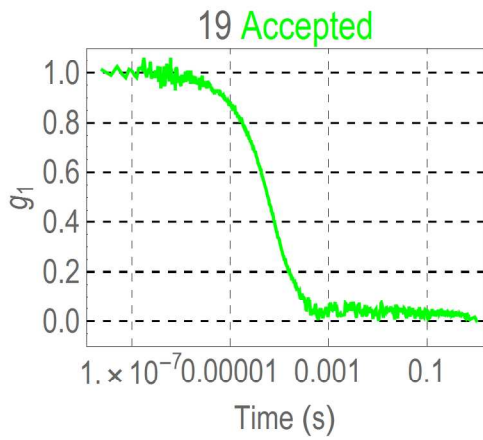


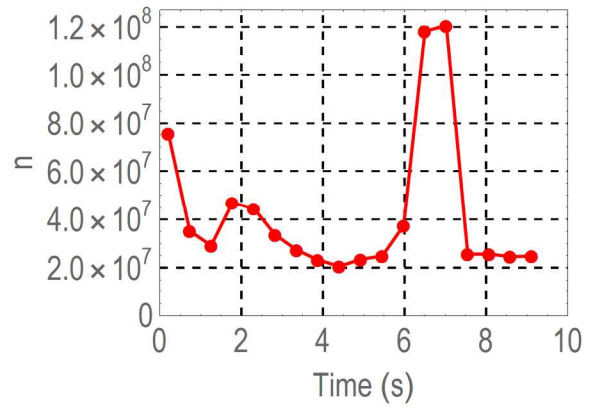
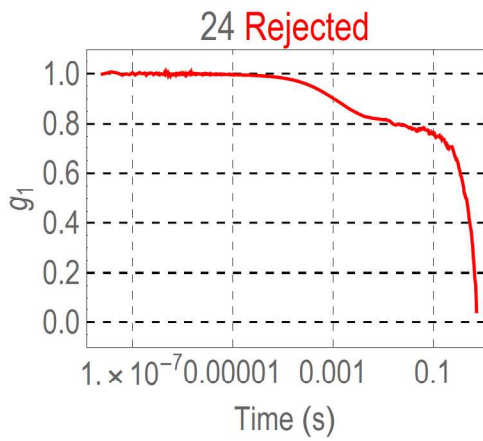
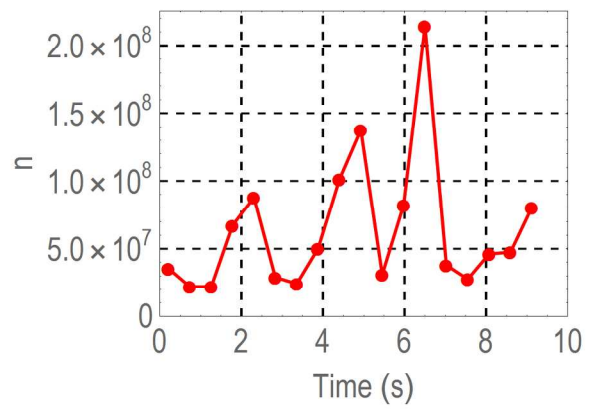
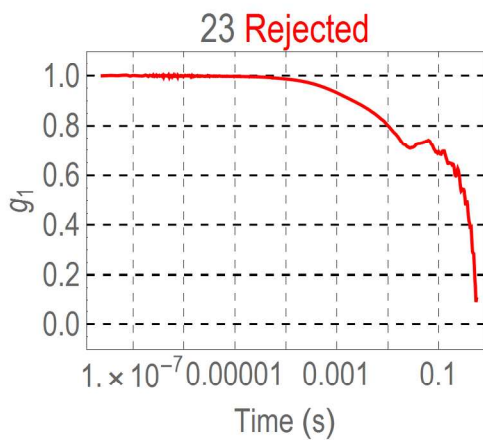
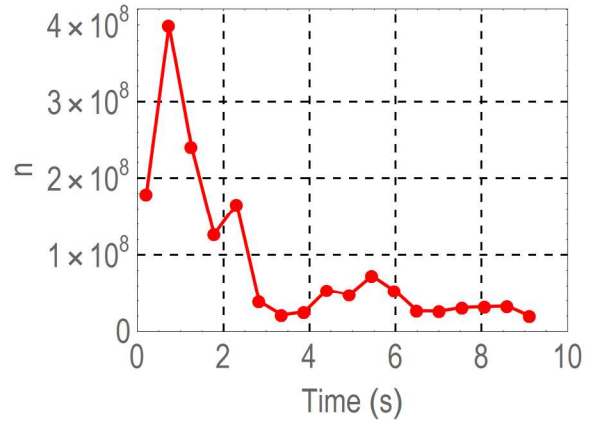
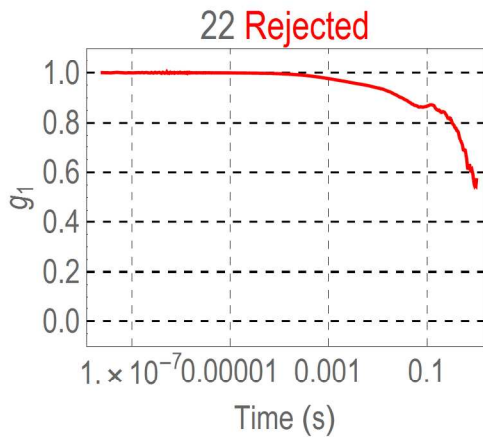


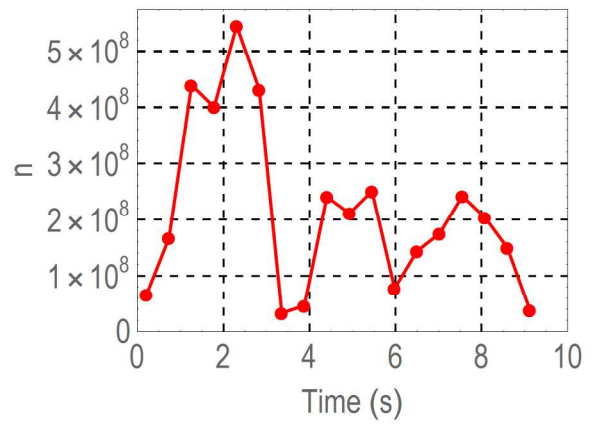
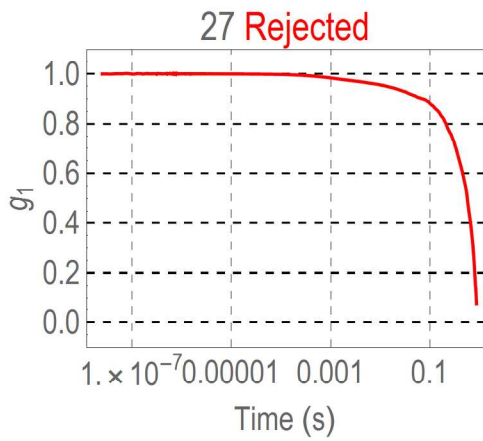
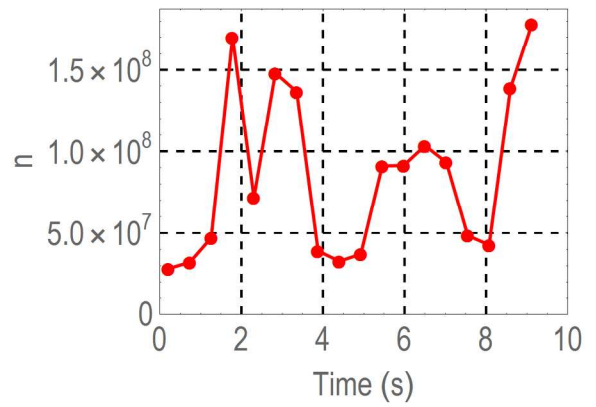
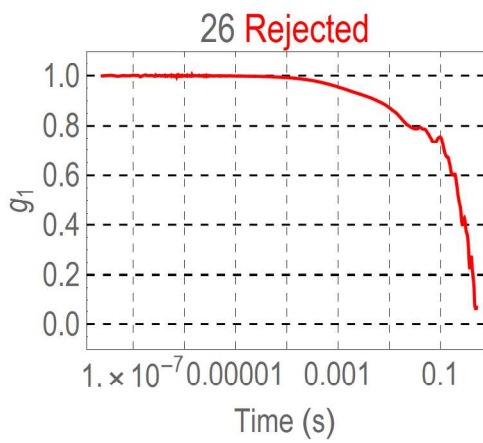
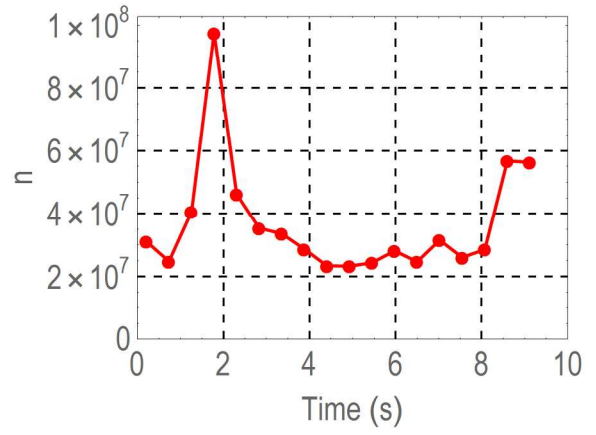
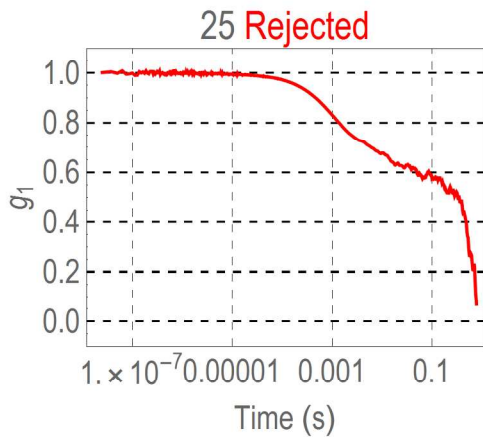


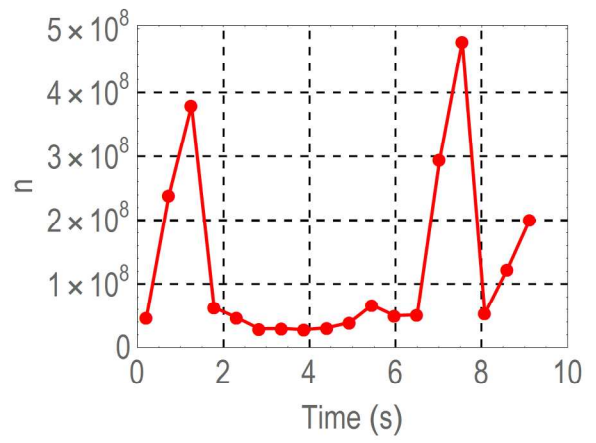
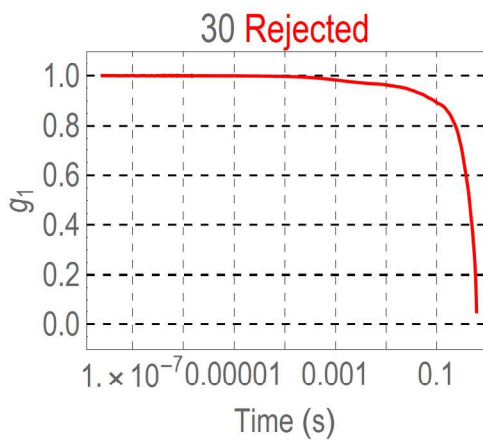
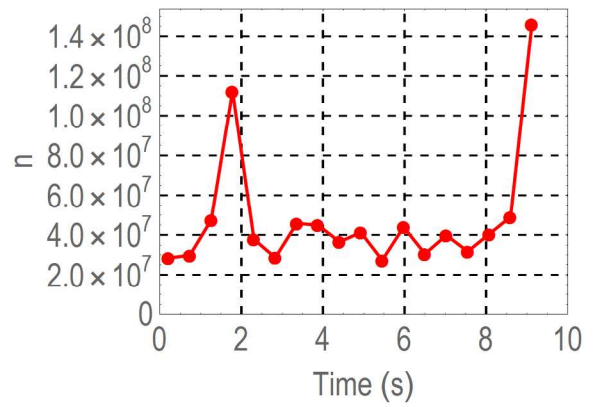
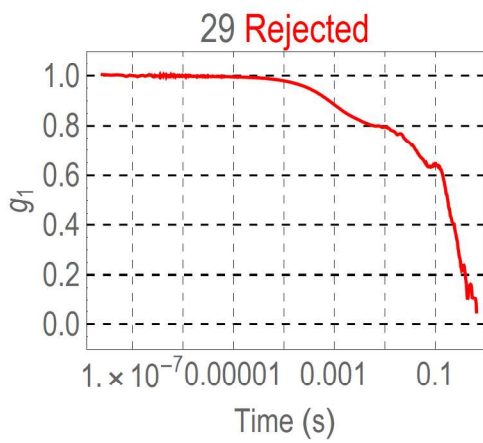
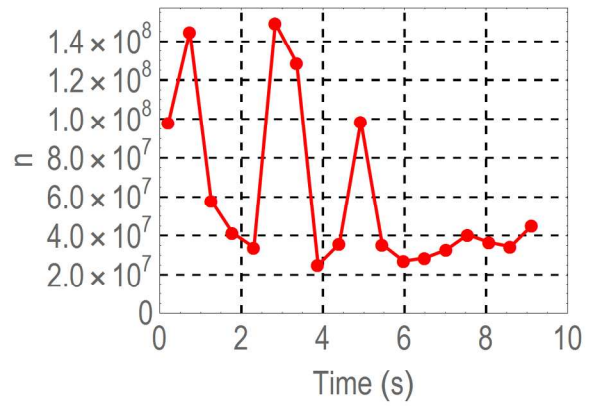
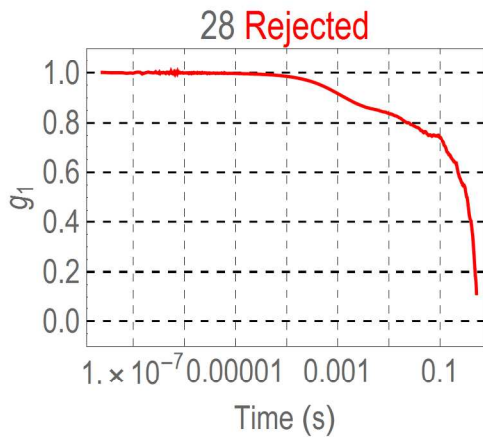


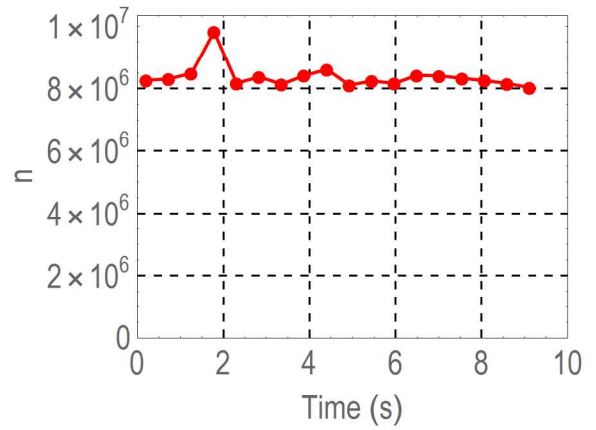
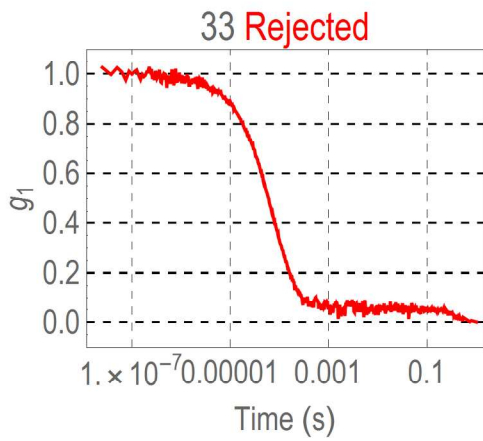
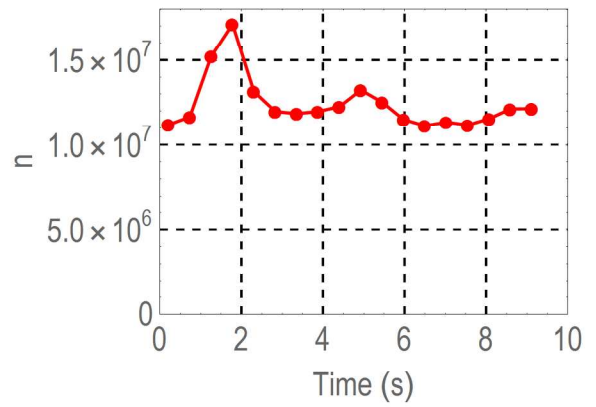
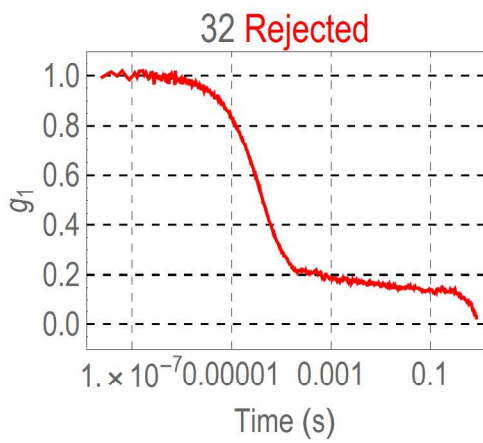
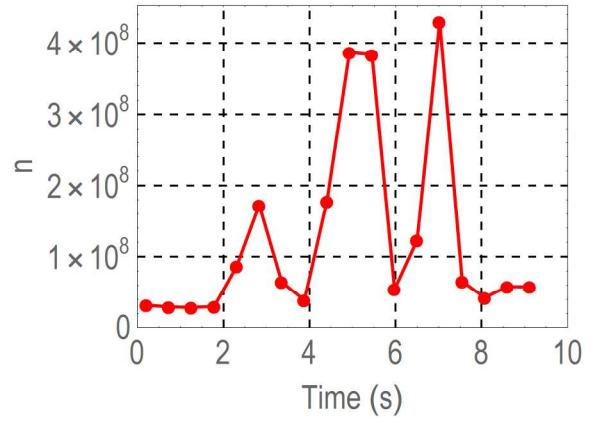
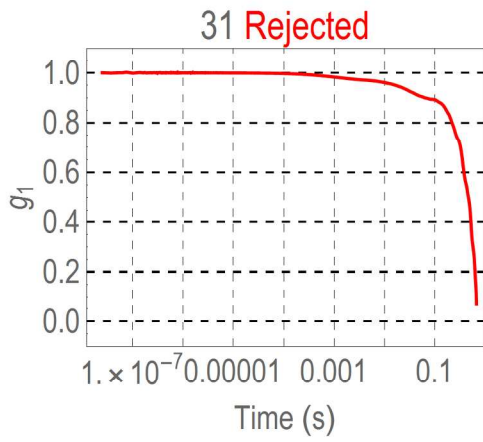


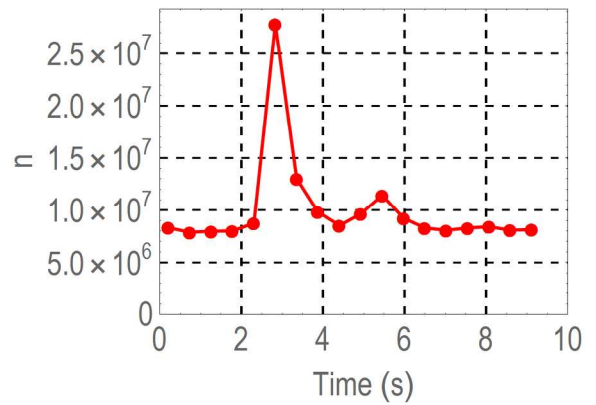
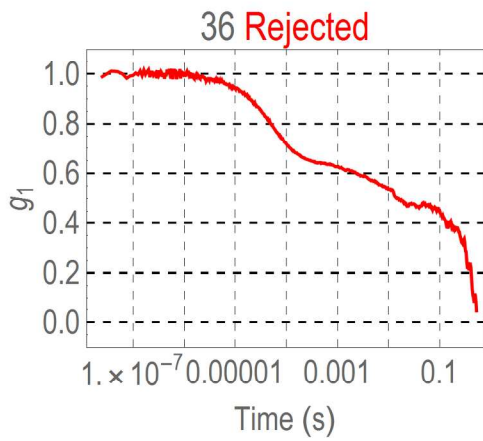
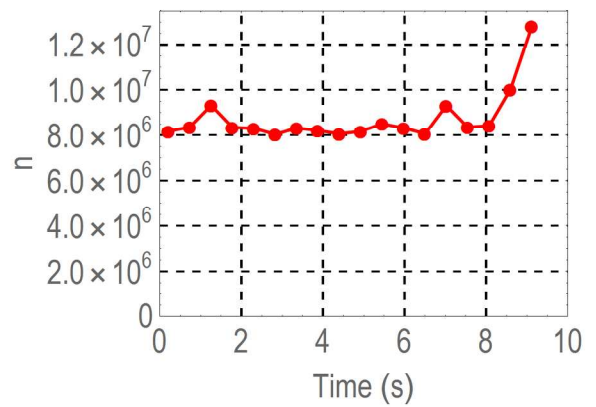
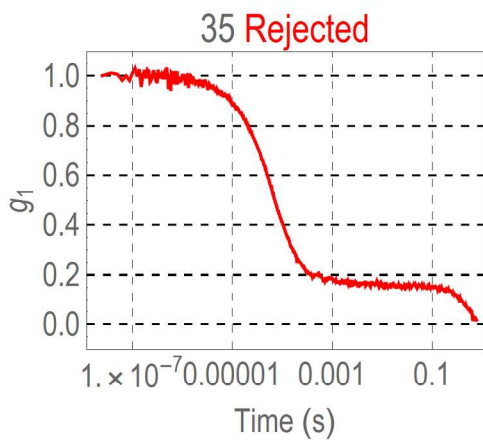
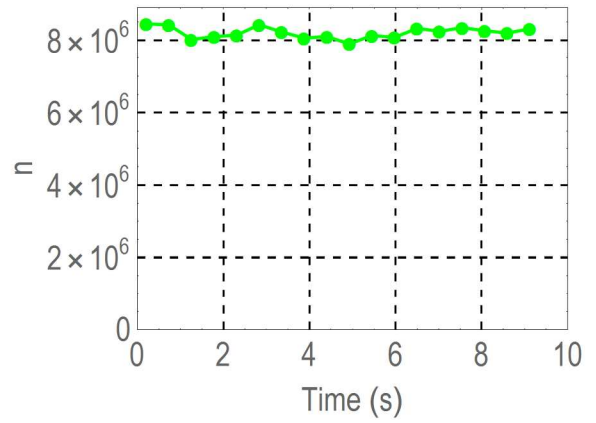
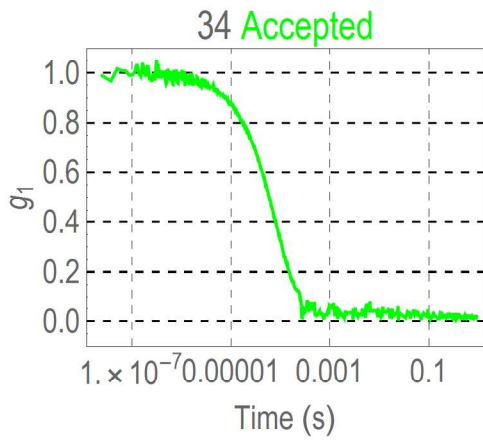


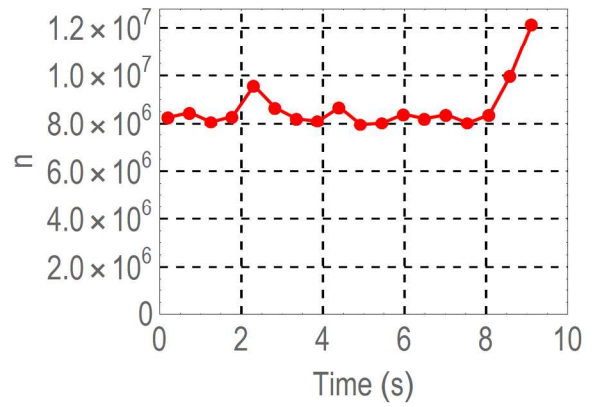
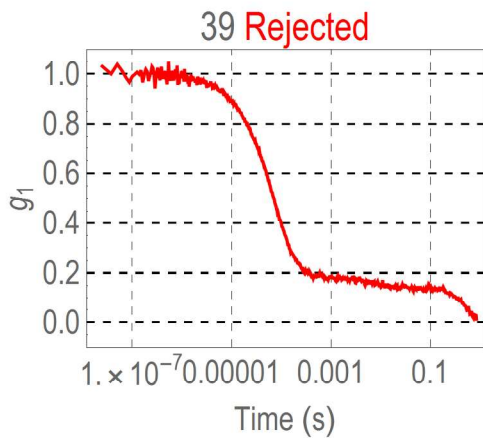
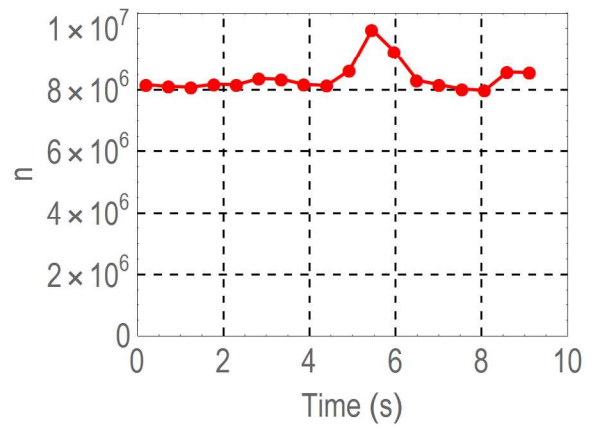
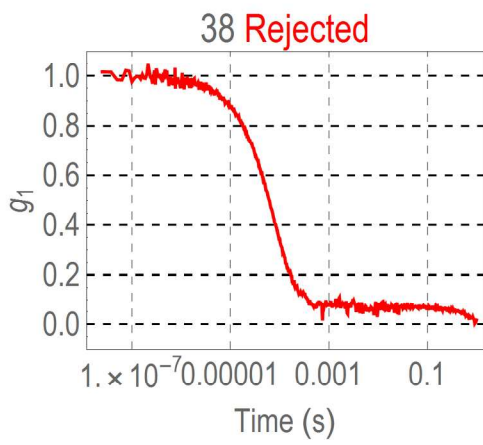
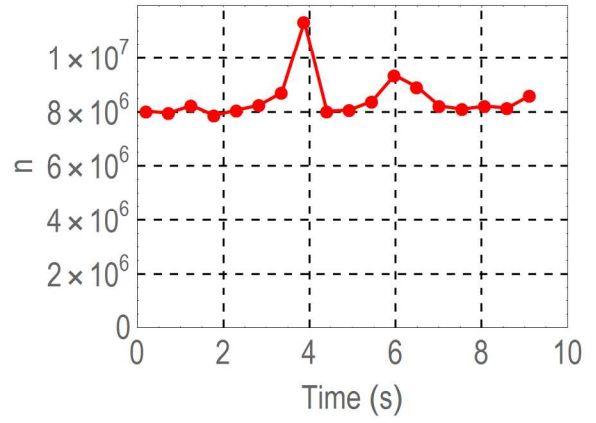
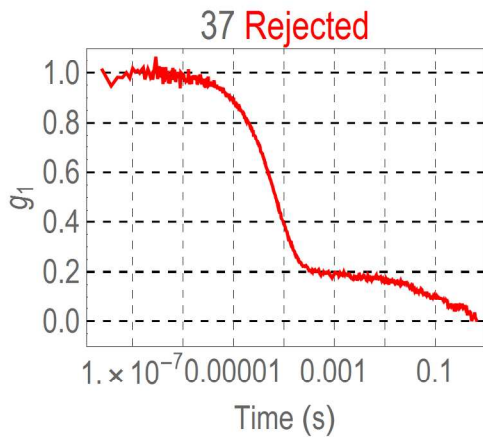


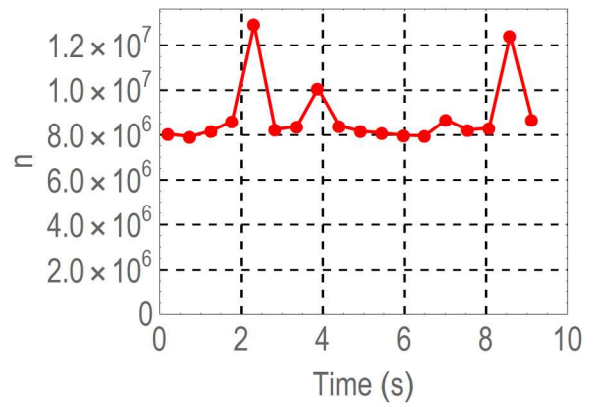
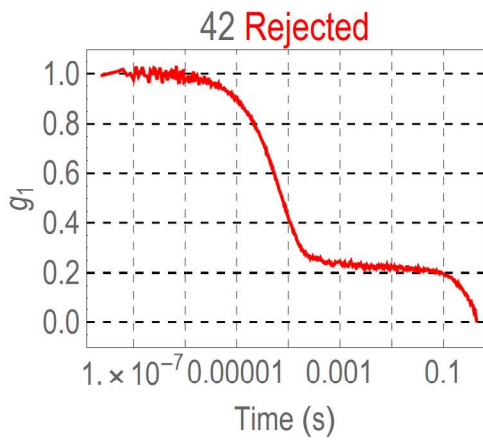
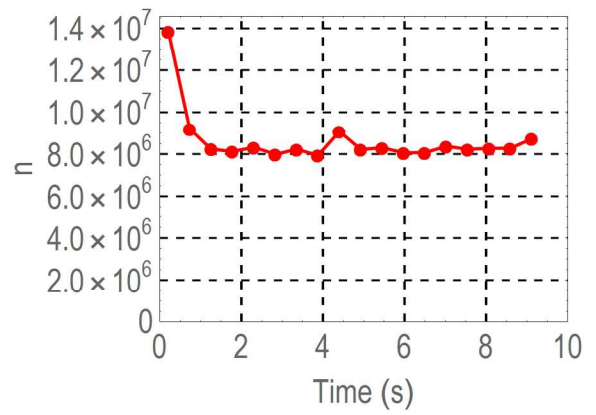
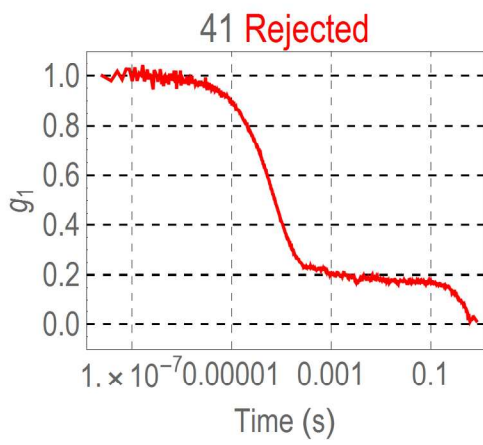
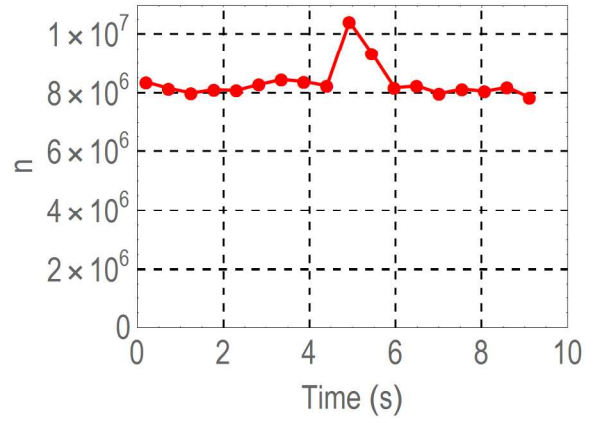
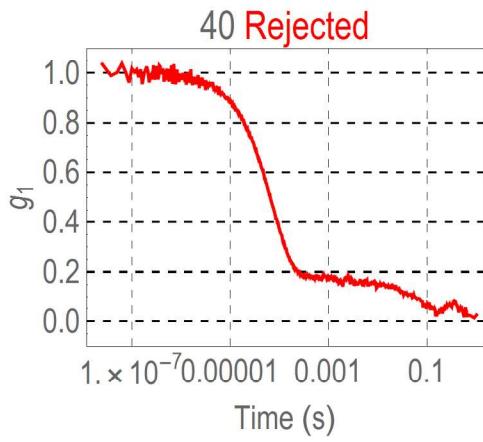


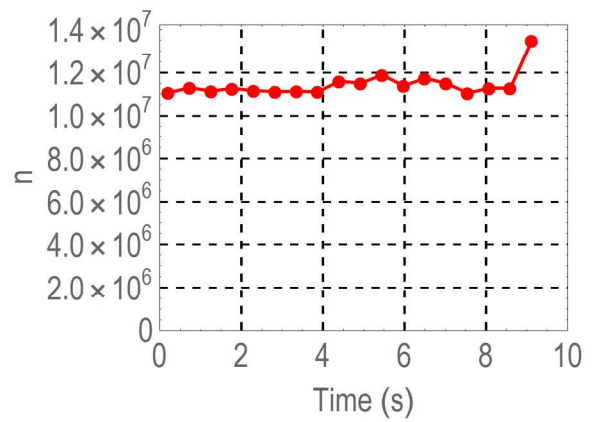
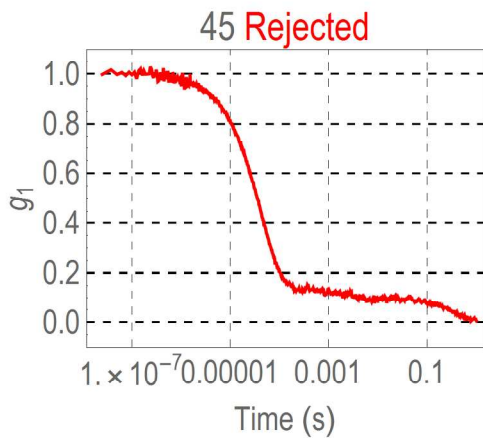
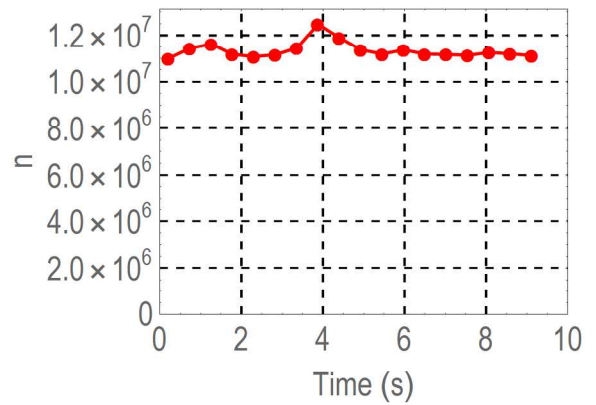
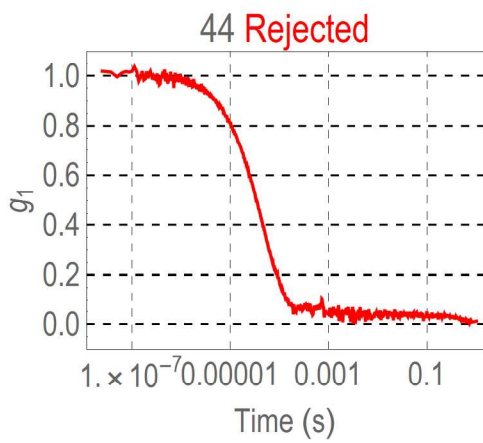
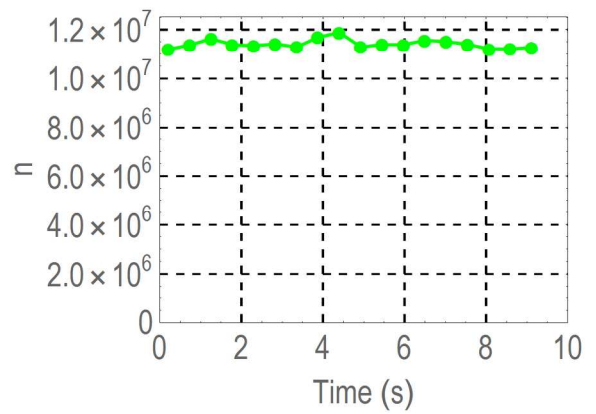
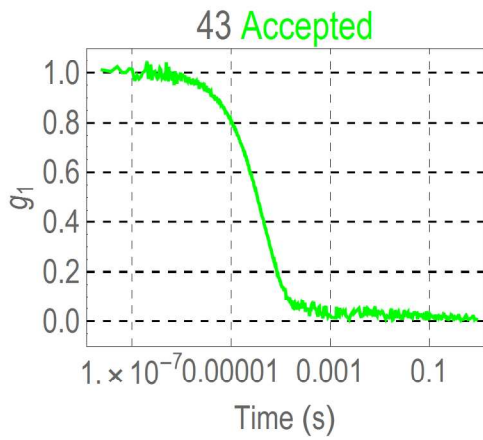


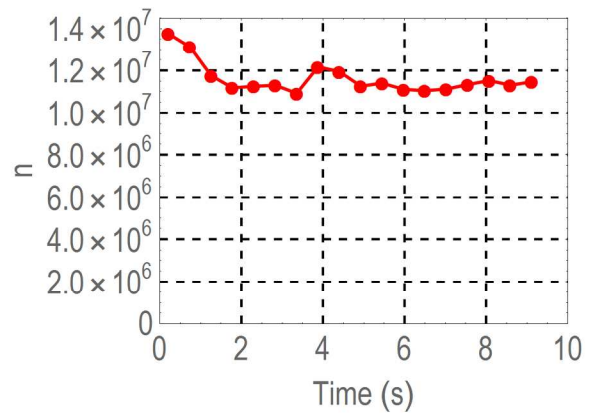
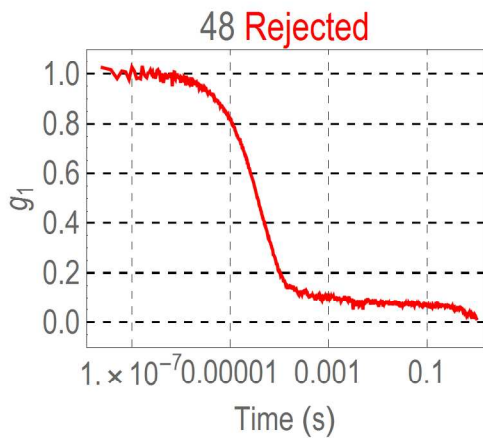
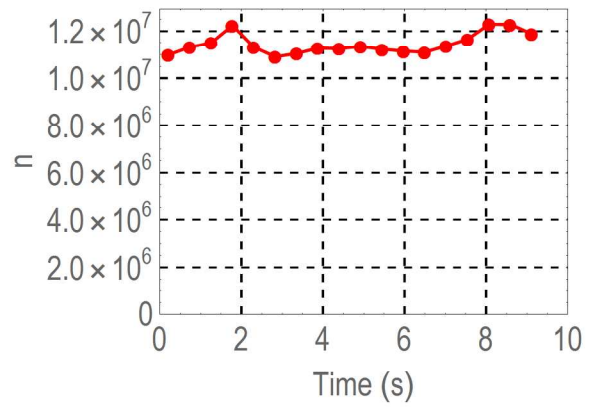
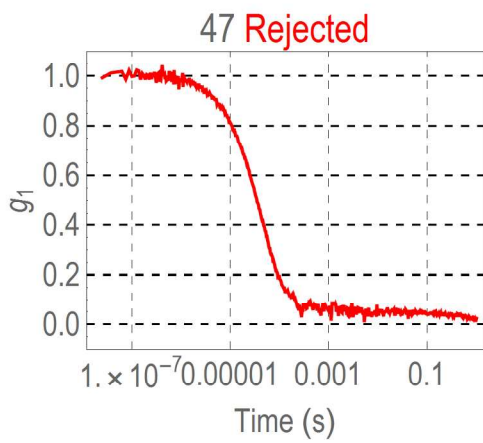
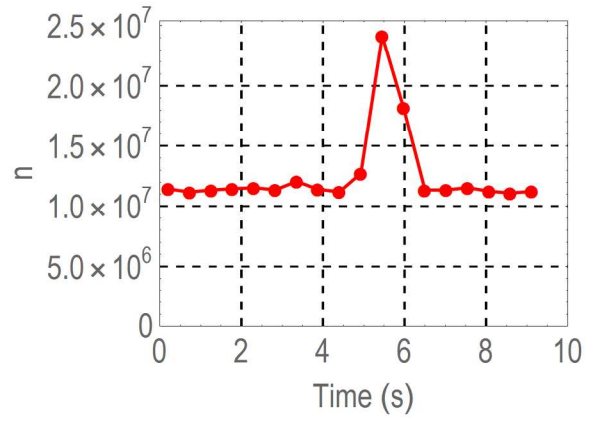
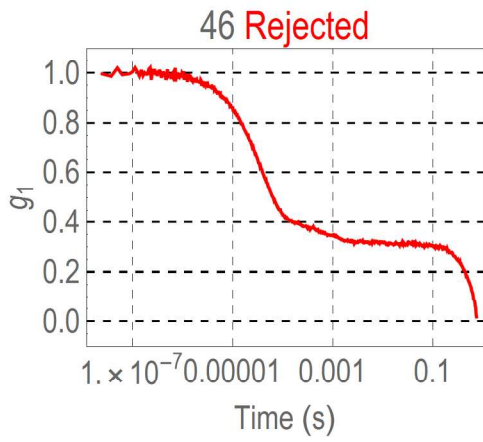


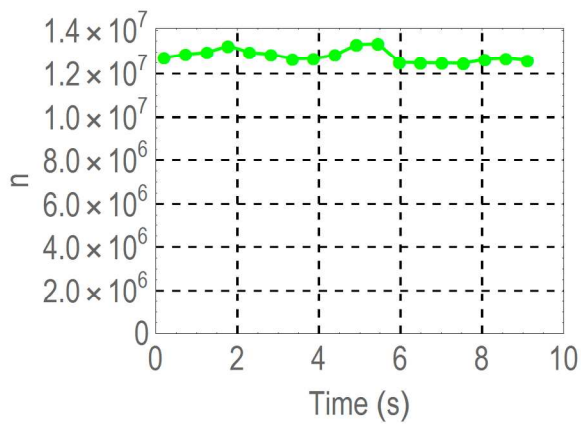
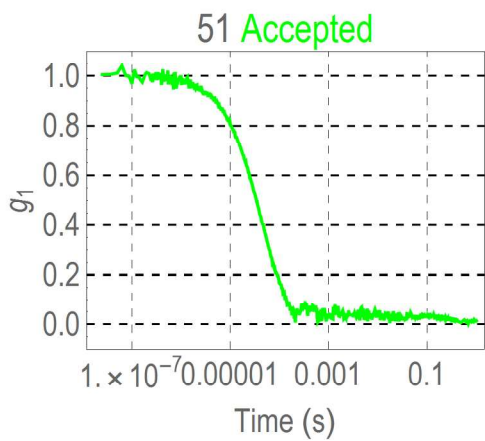
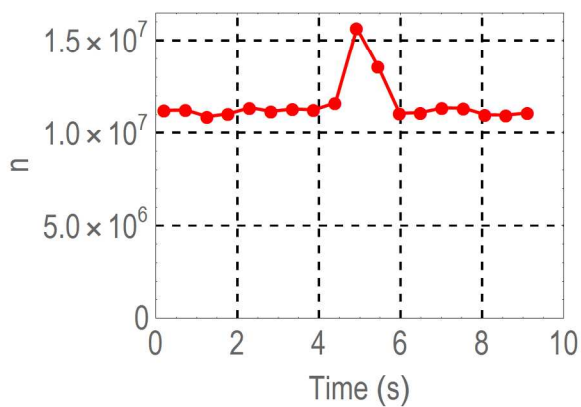
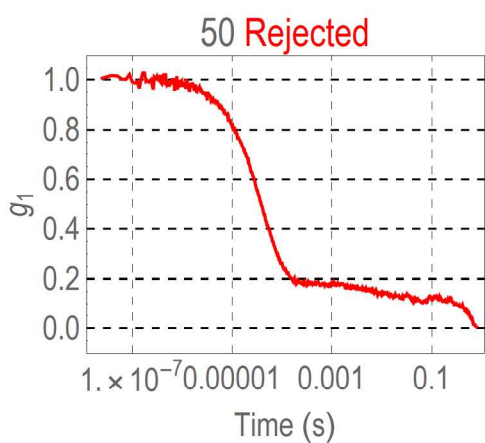
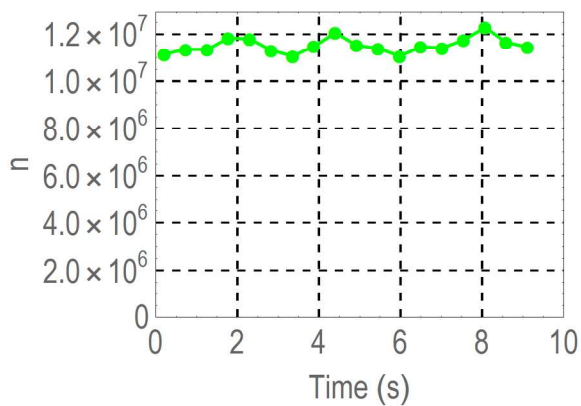
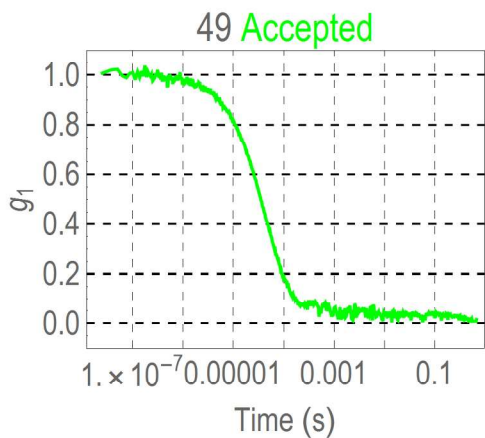


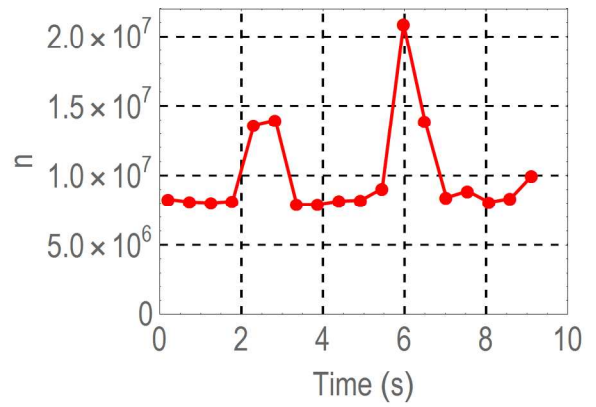
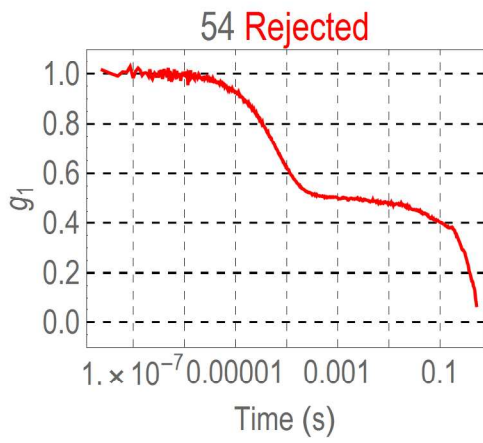
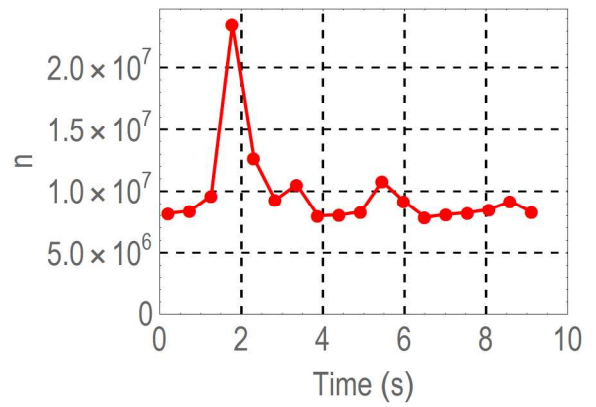
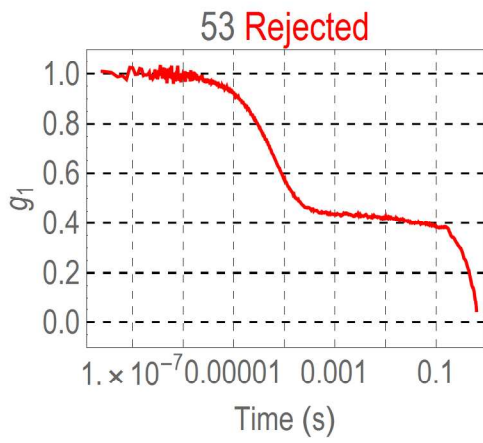
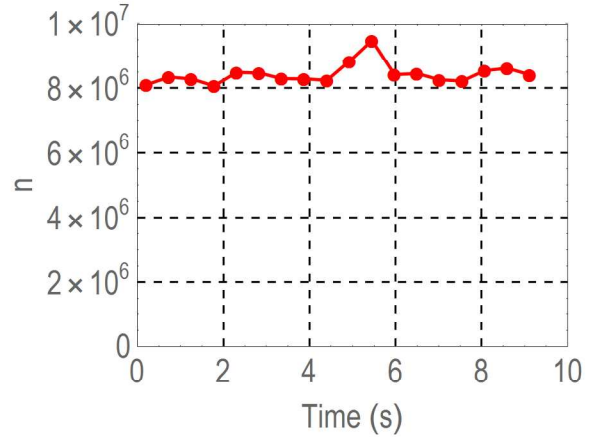
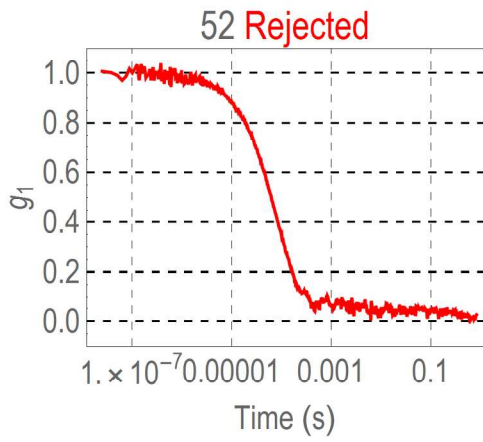


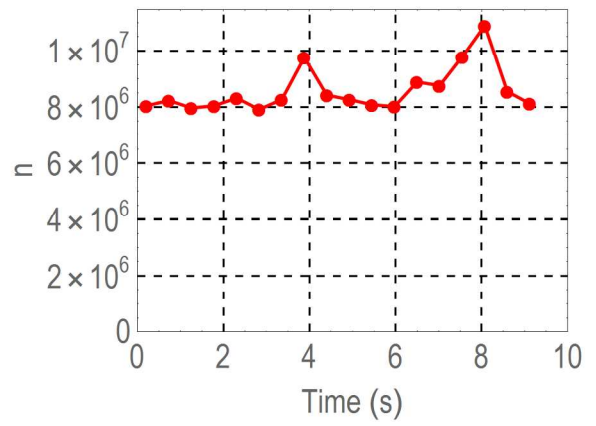
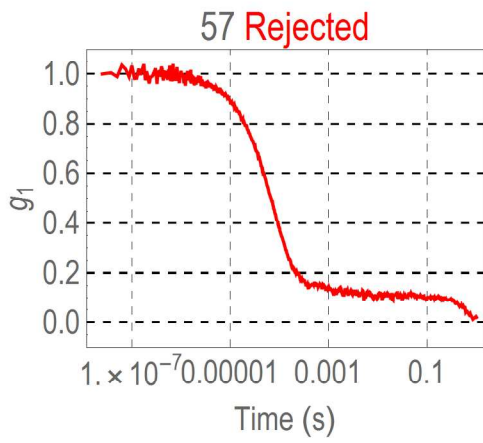
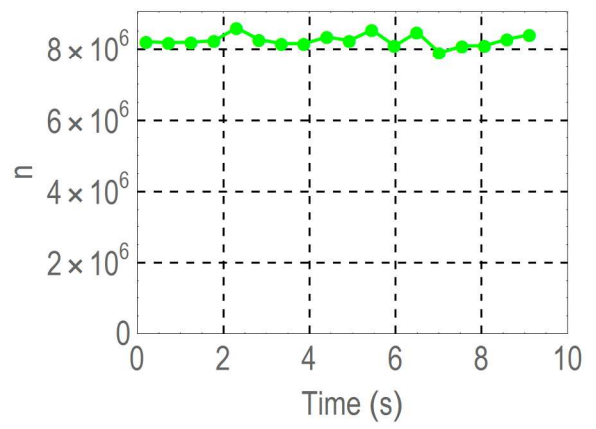
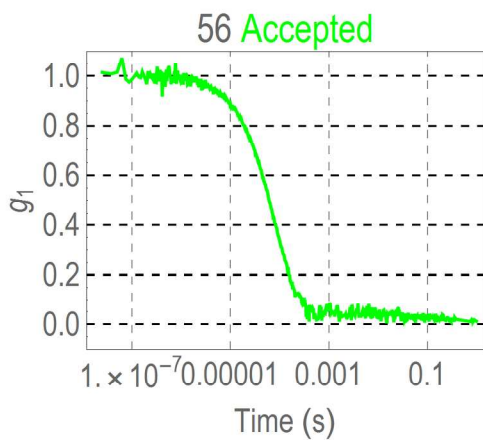
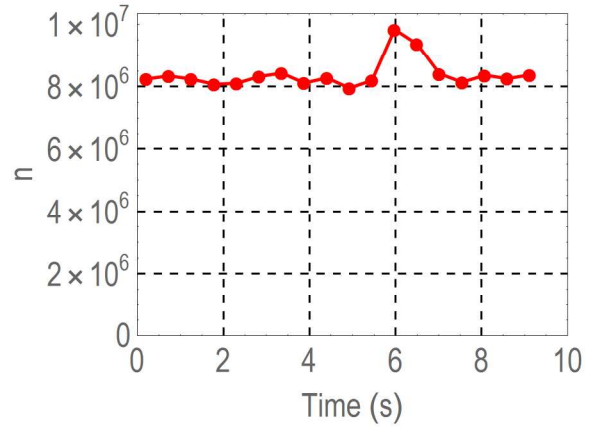
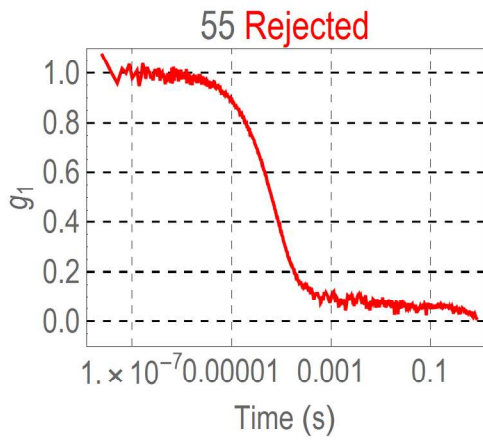


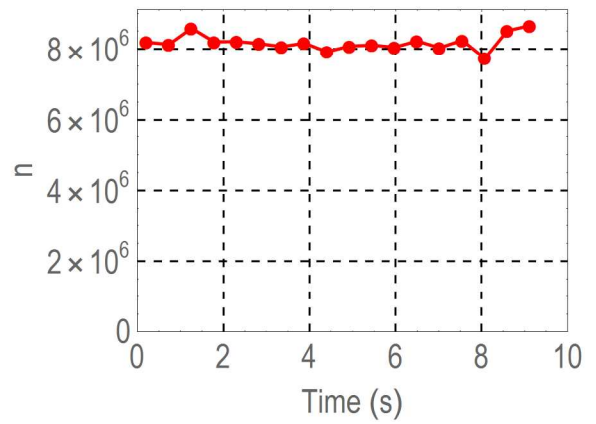
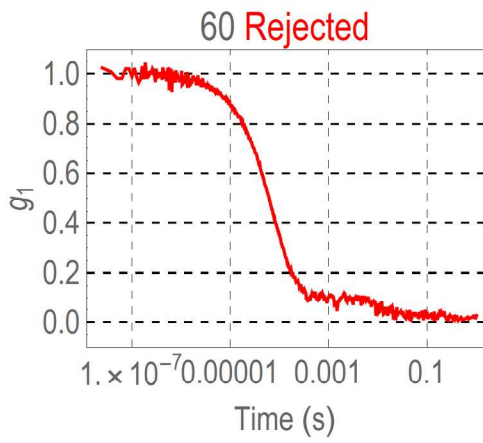
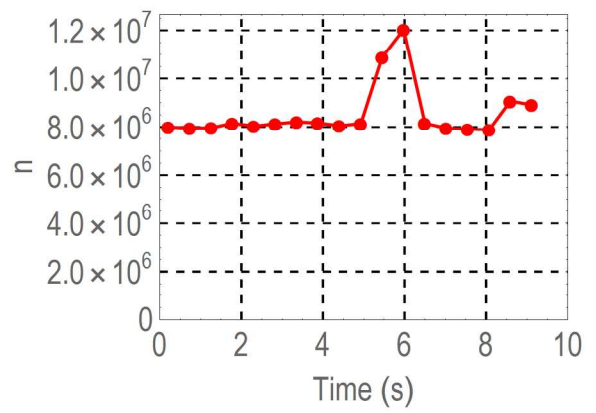
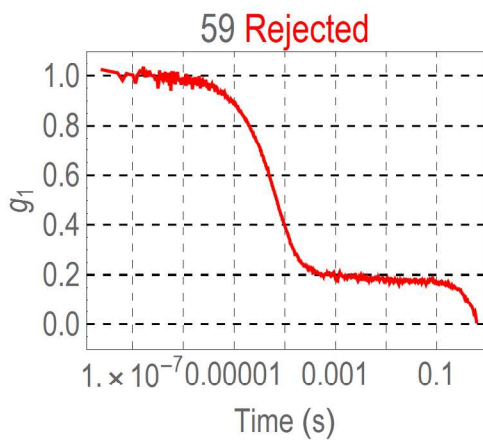
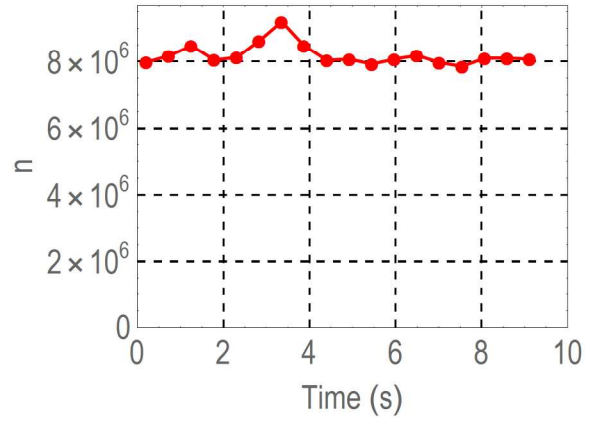
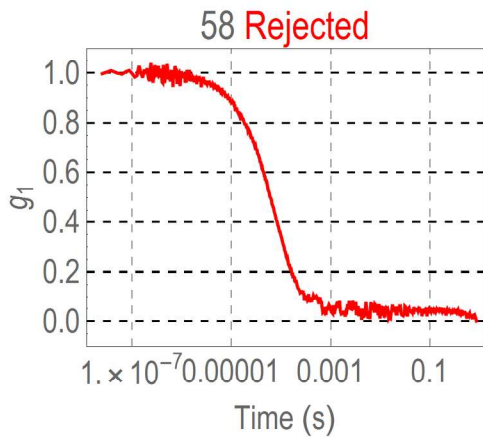


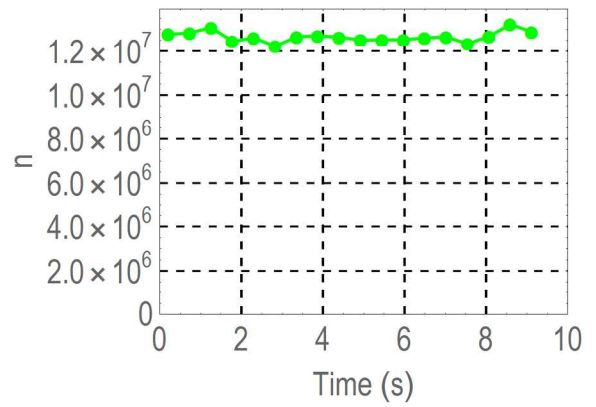
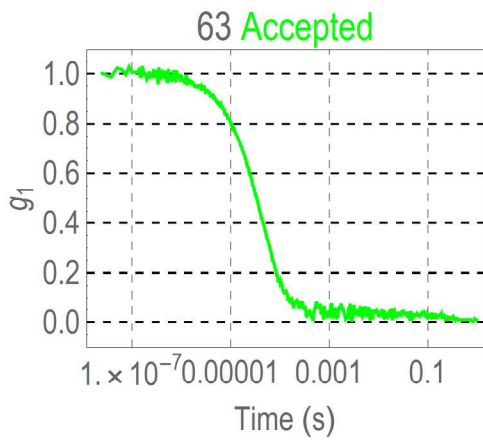
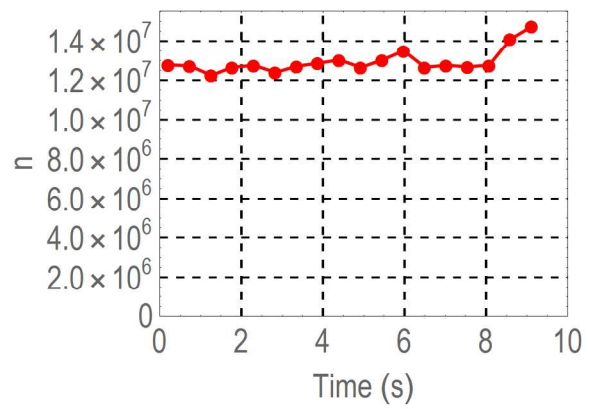
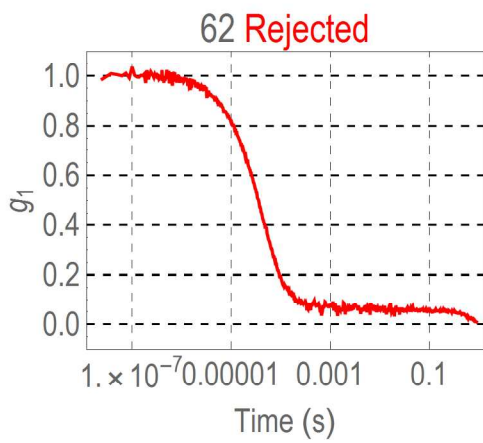
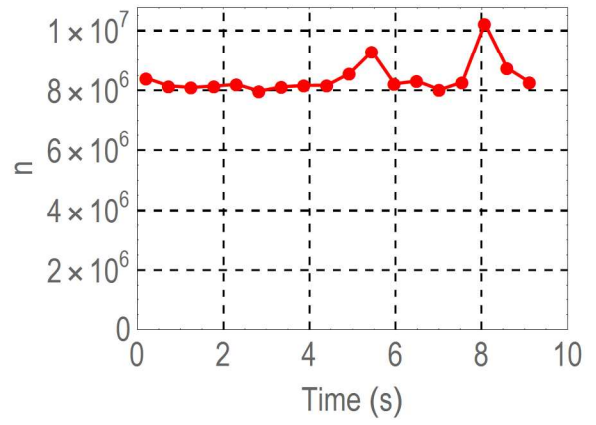
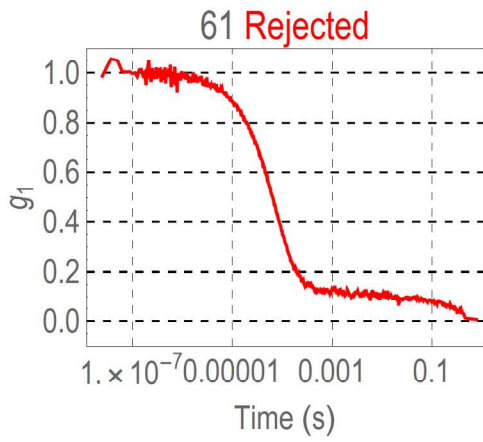


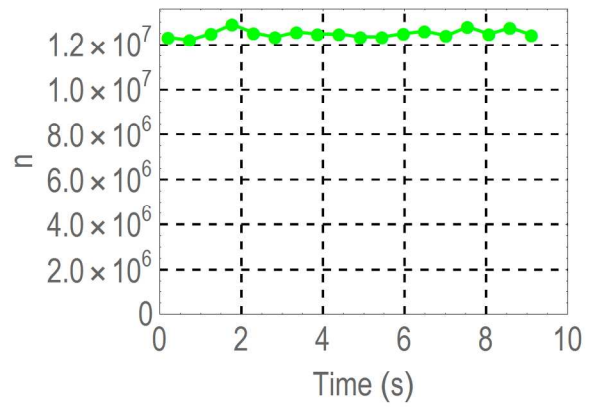
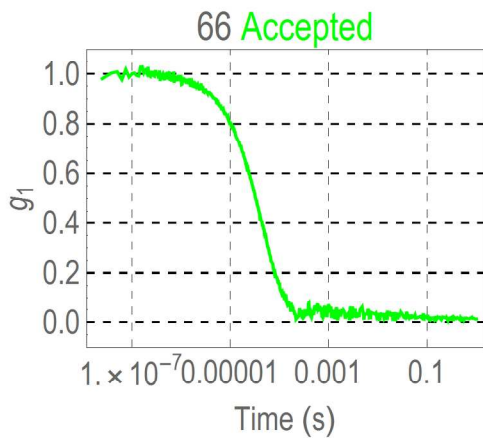
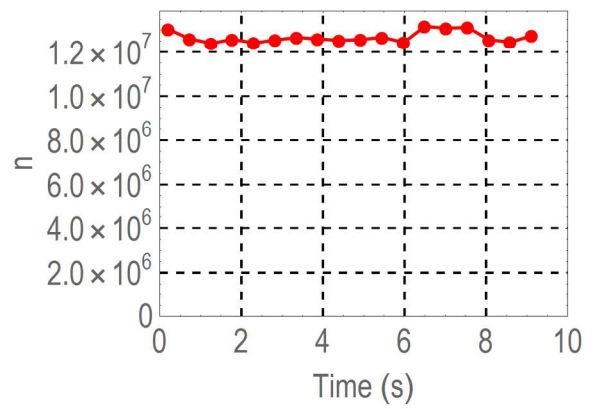
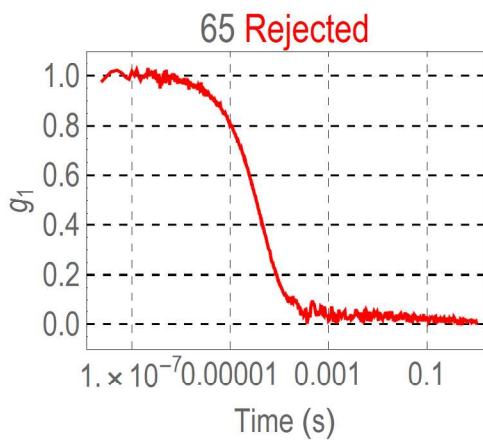
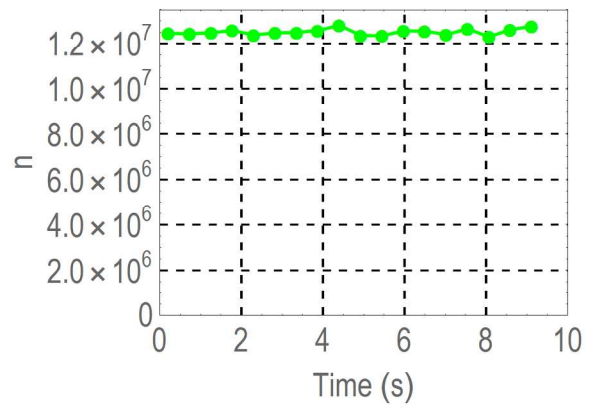
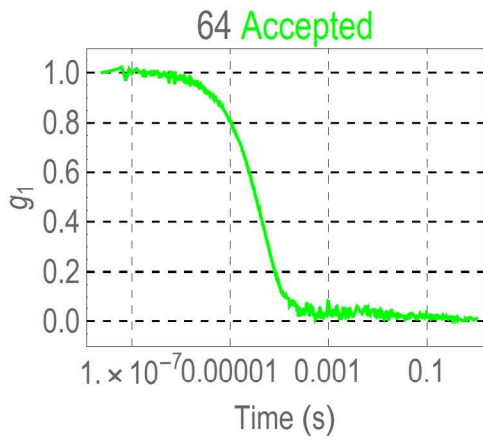


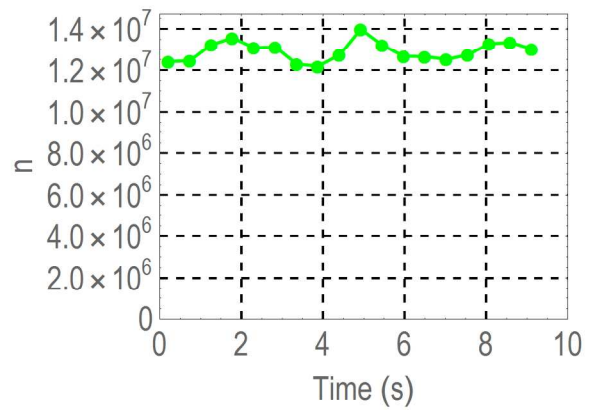
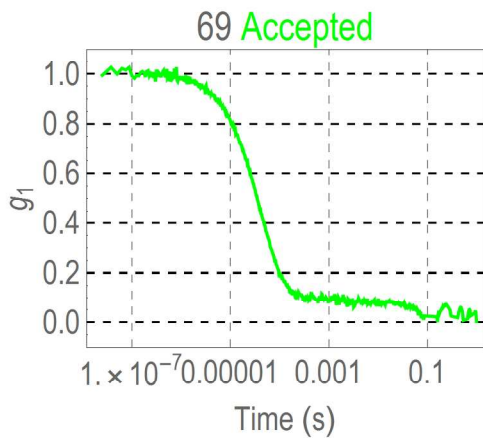
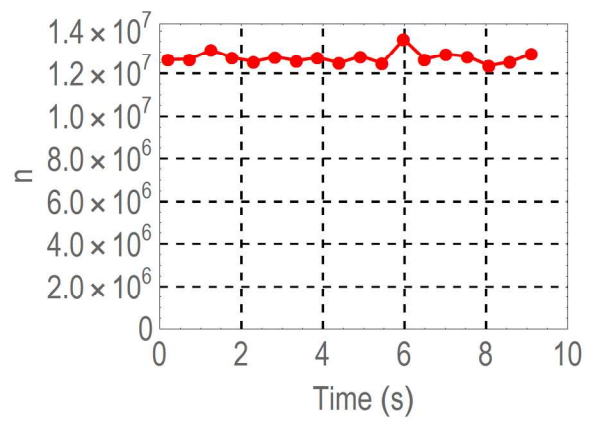
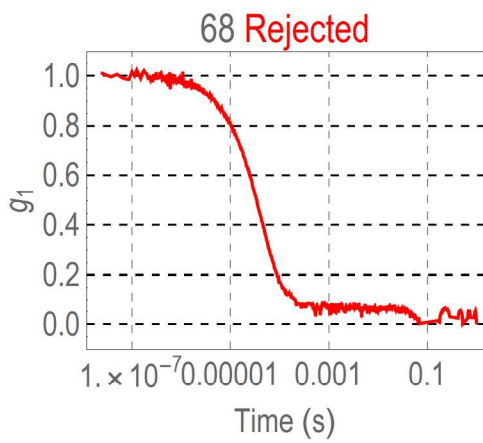
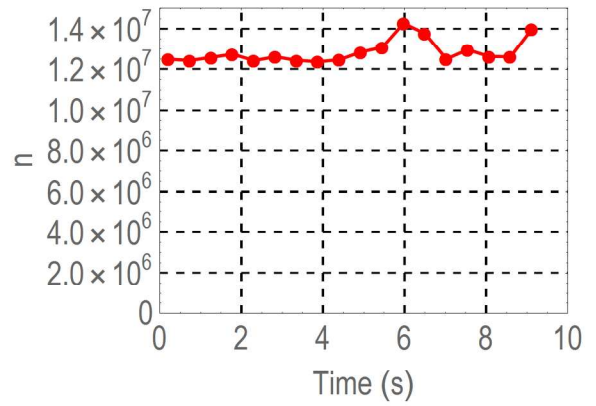
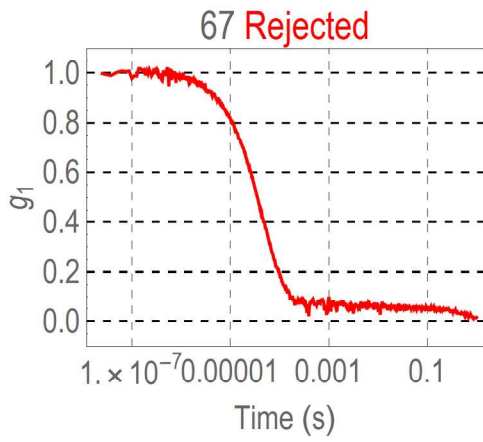


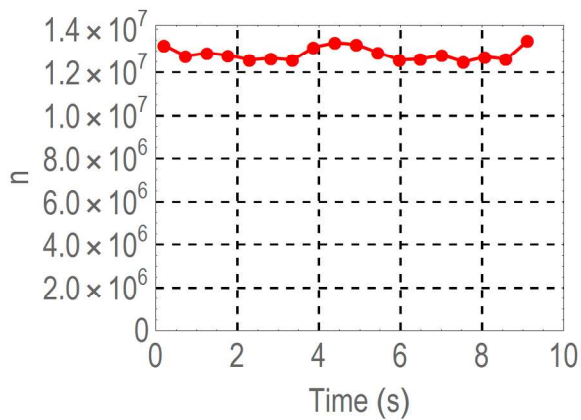
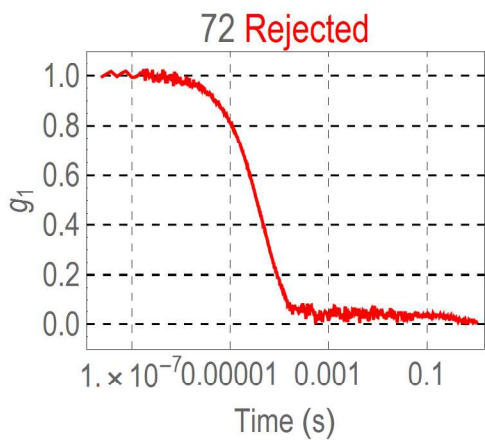
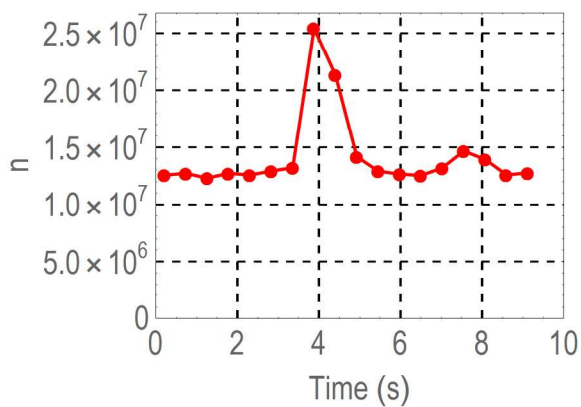
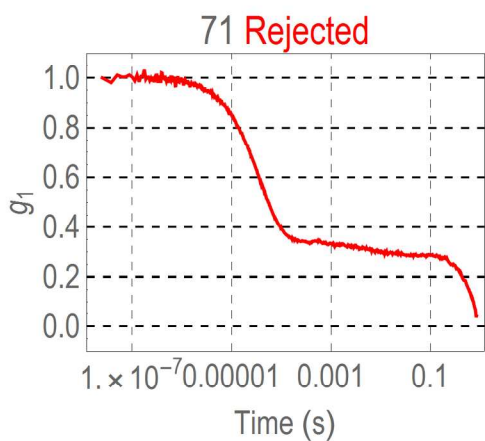
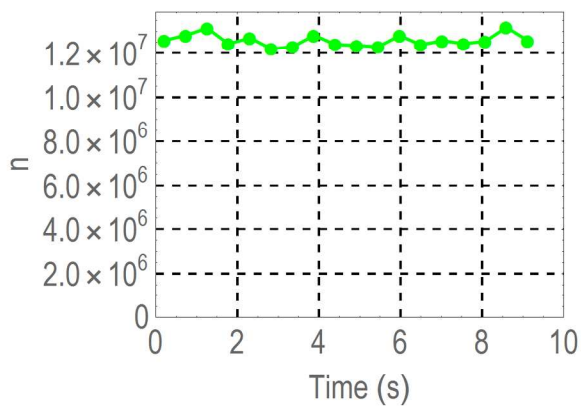
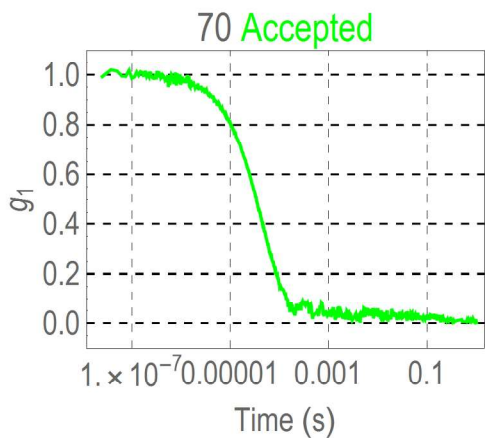


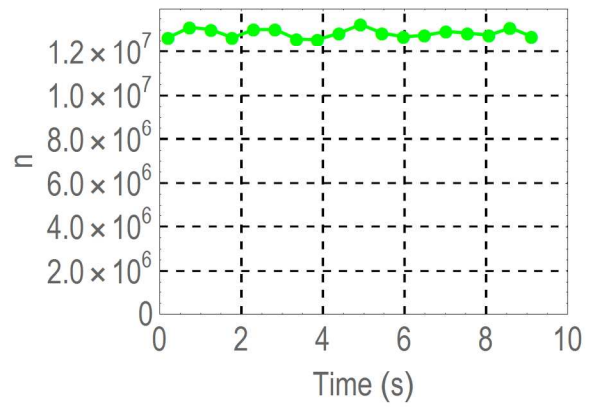
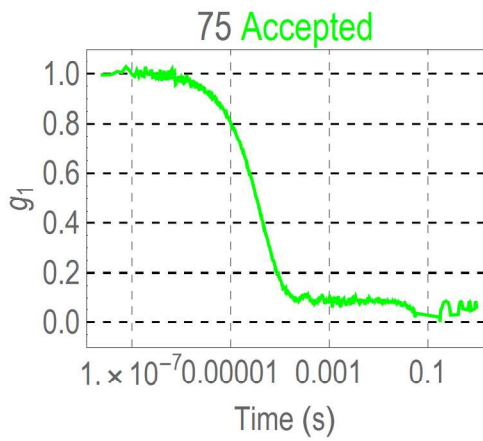
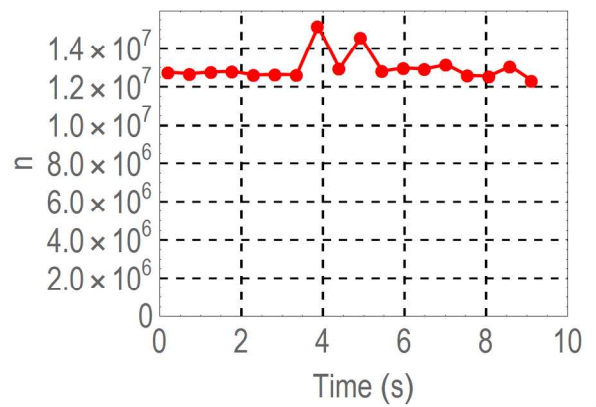
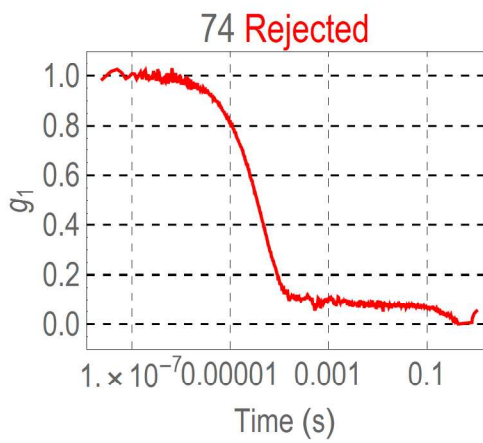
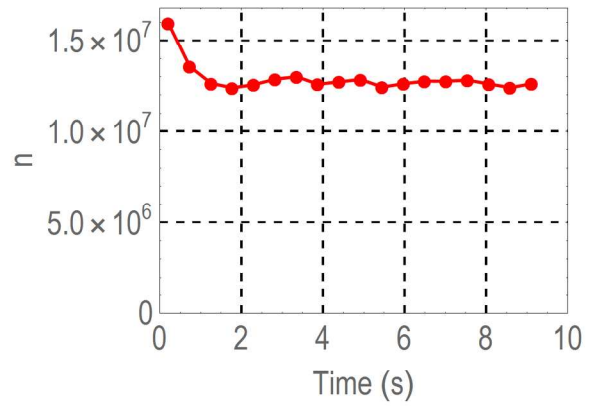
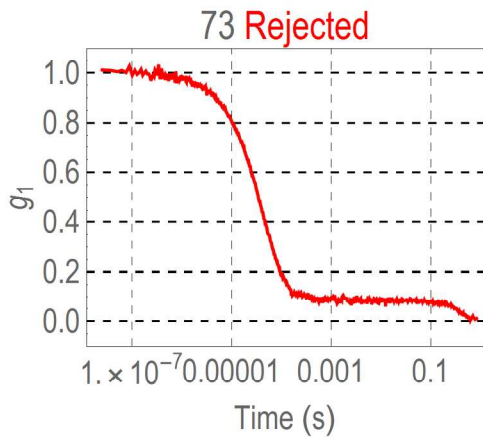


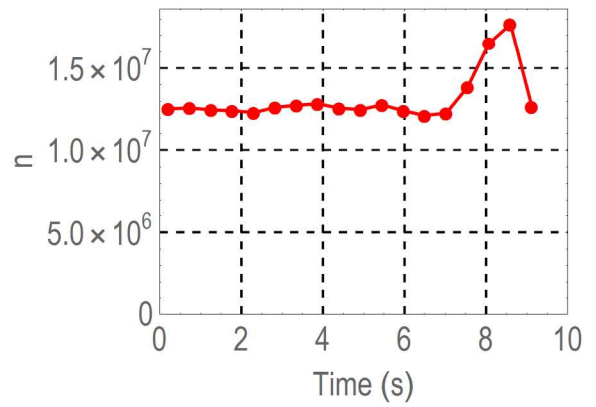
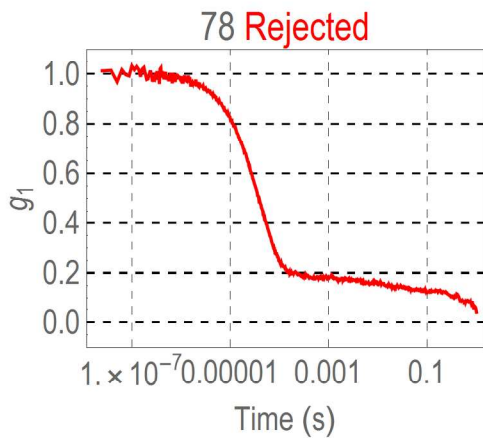
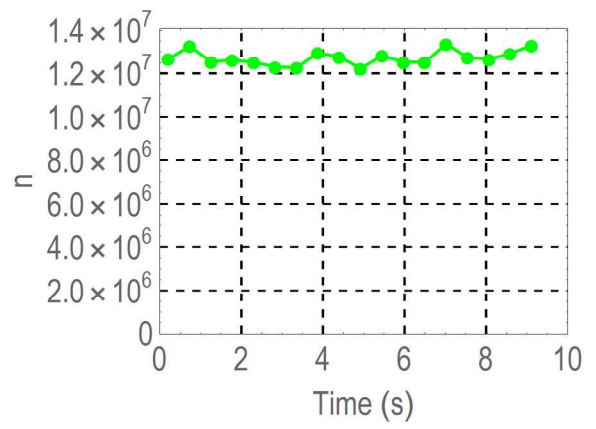
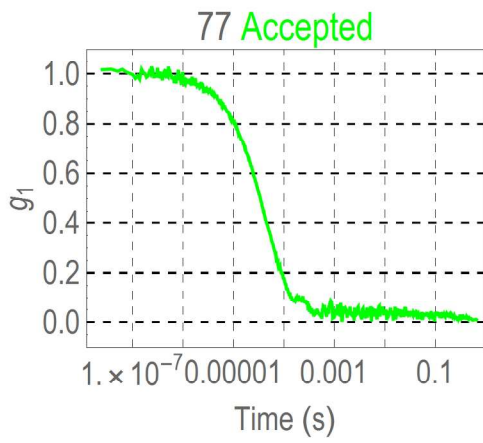
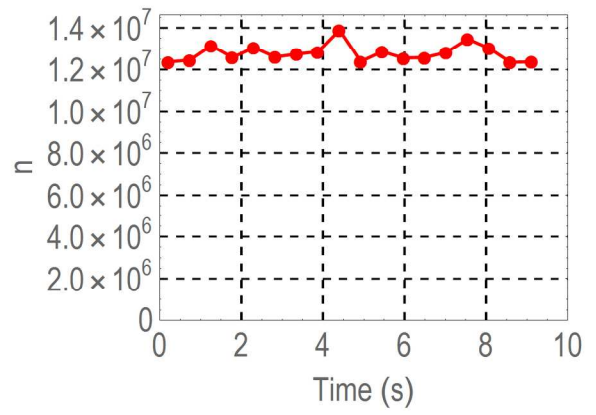
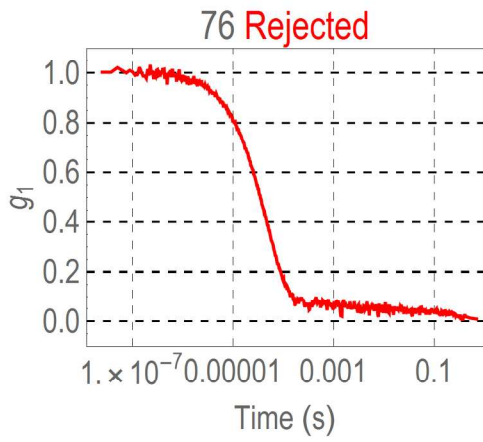


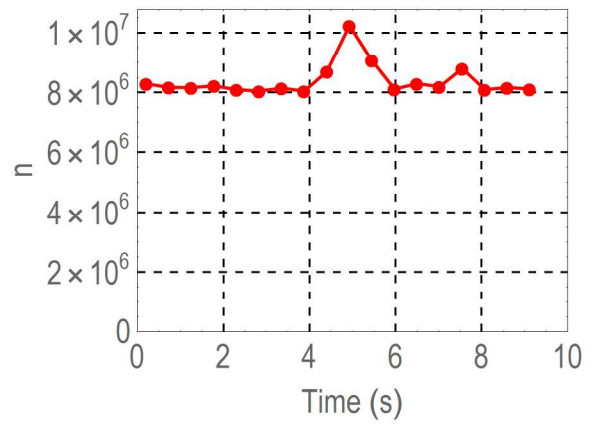
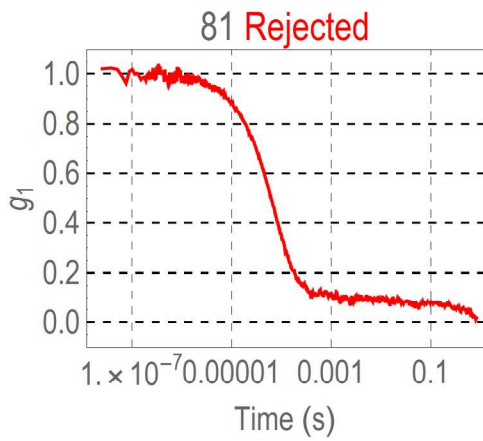
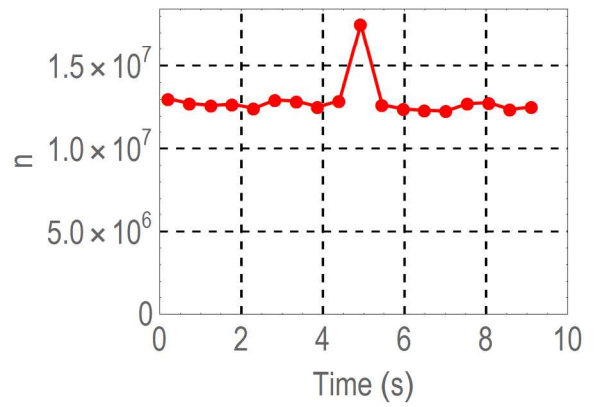
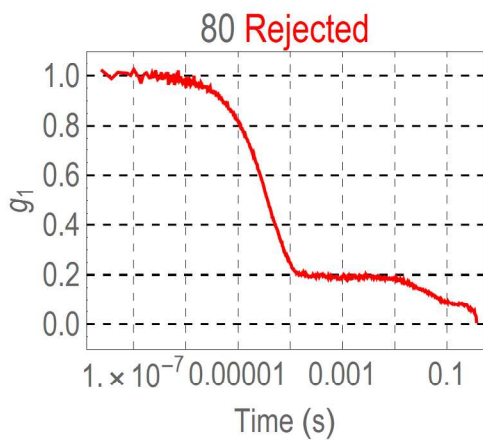
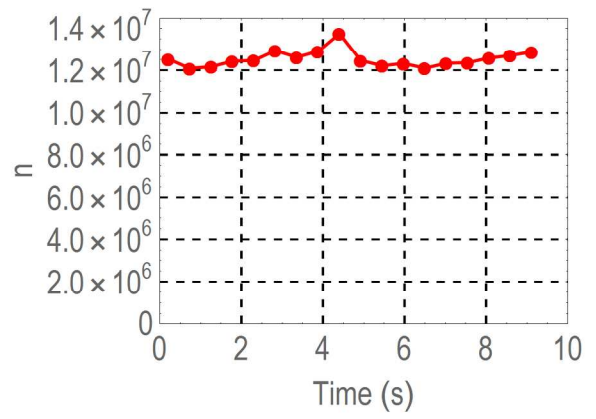
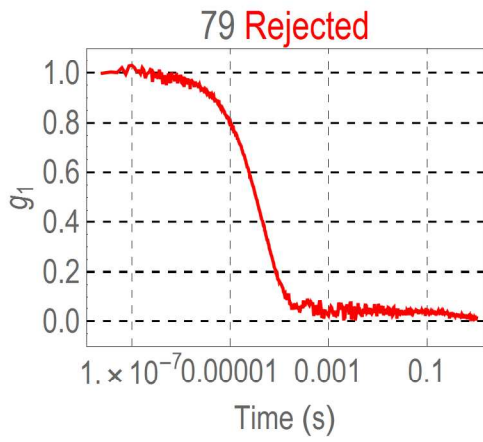


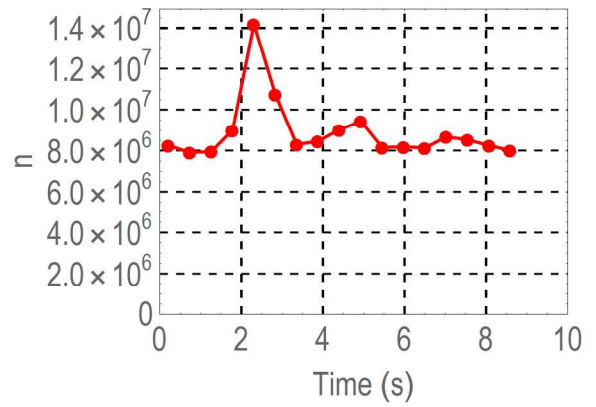
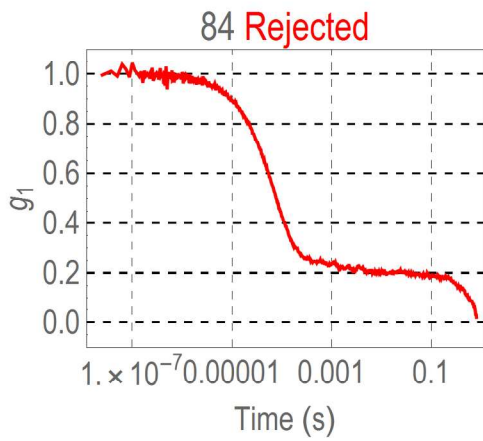
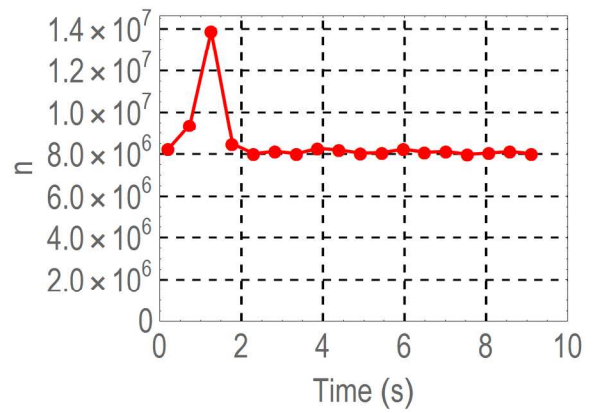
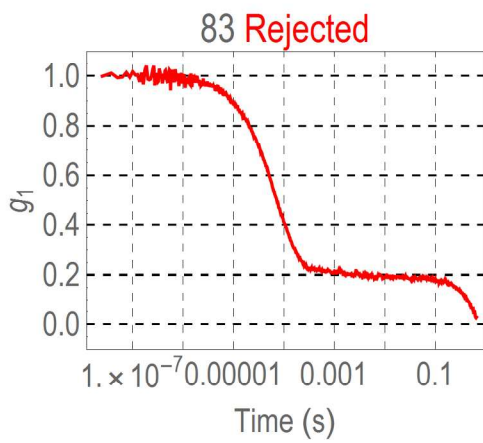
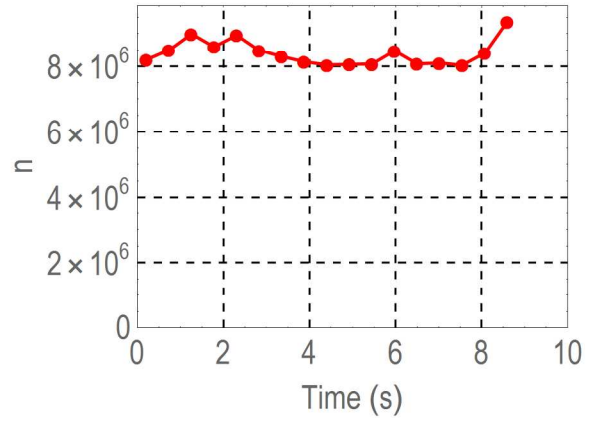
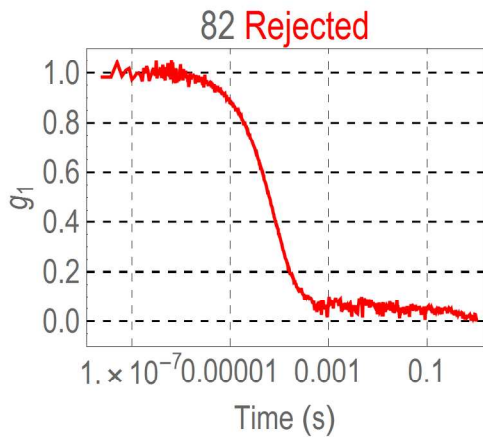


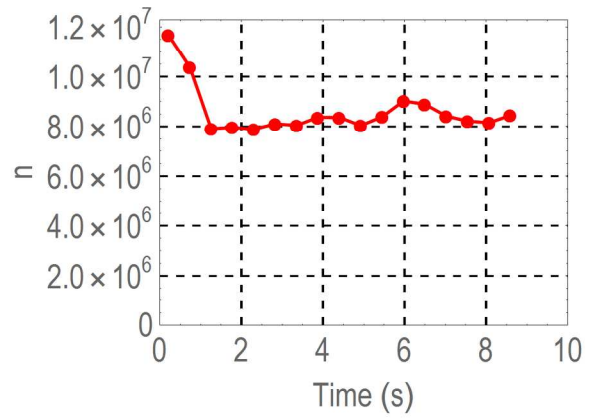
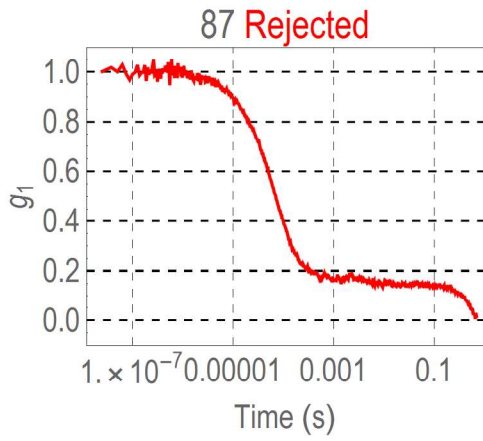
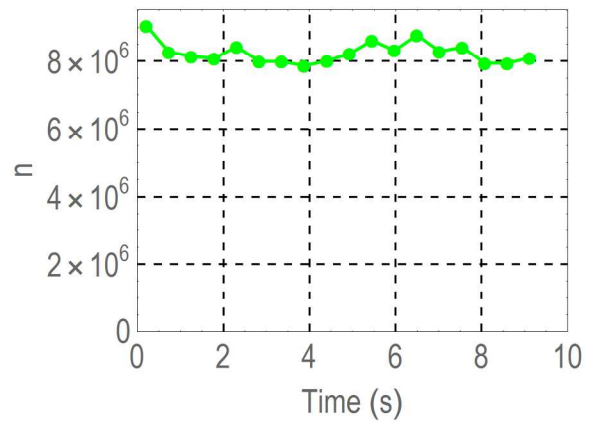
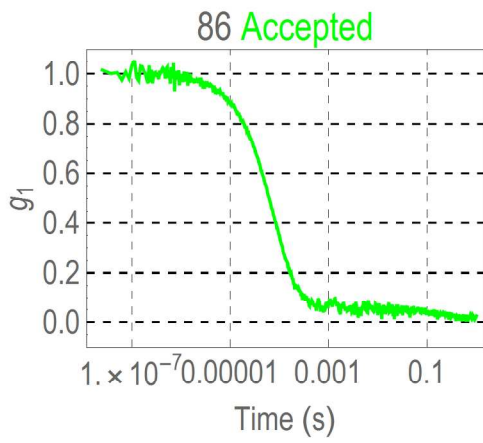
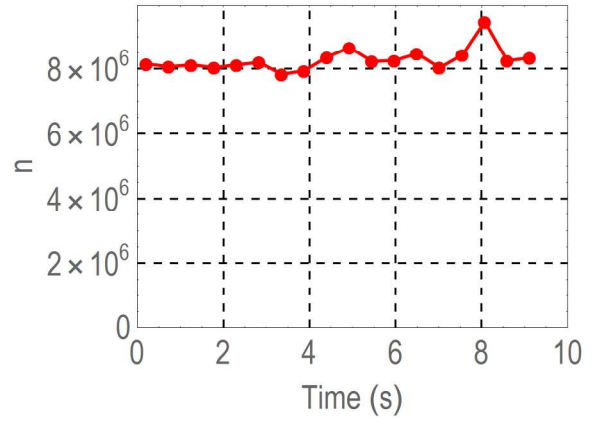
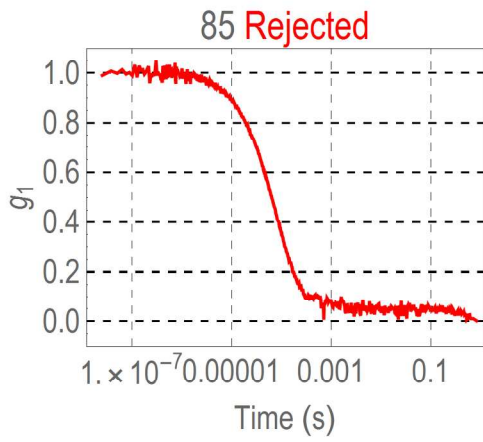


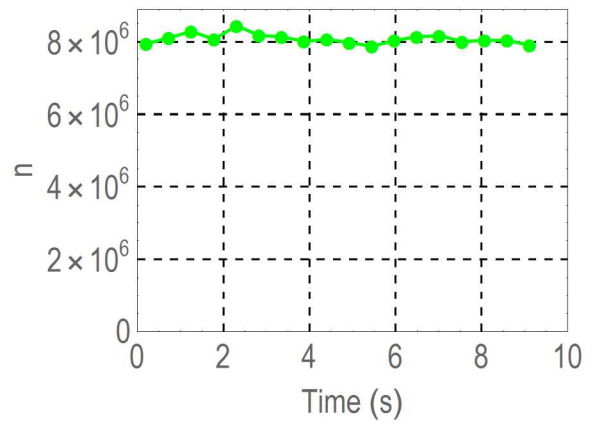
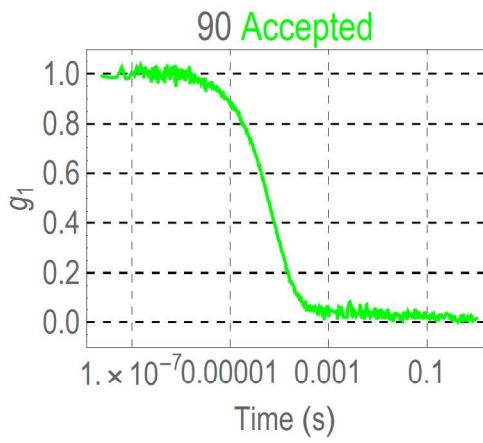
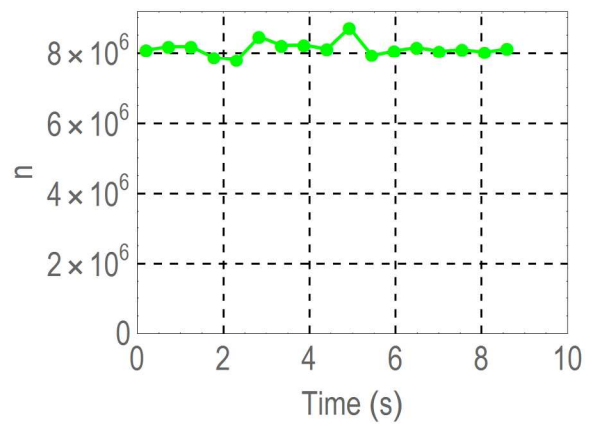
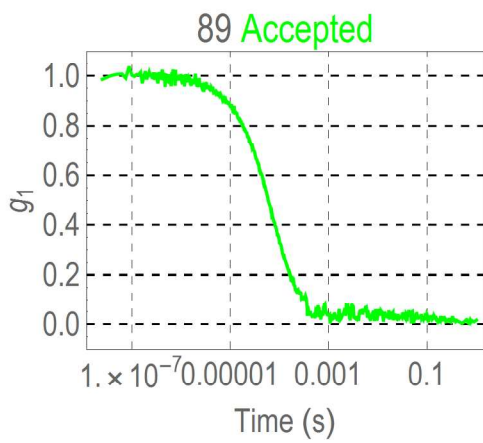
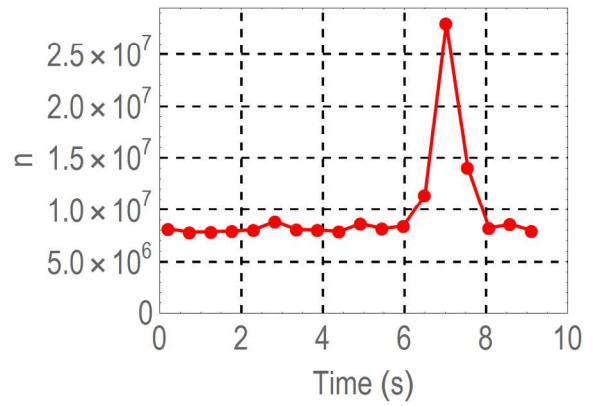
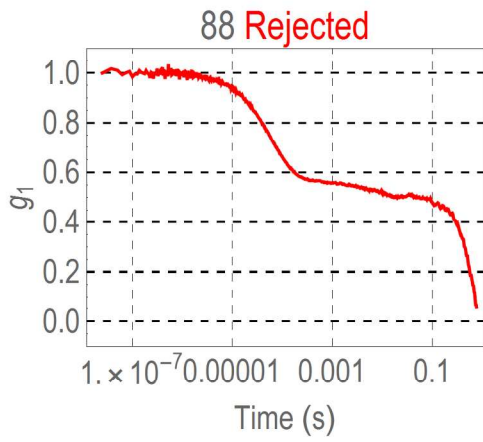












## References

- (1) Ridler, T. W.; Calvard, S. *Ieee T Syst Man Cyb* **1978**, *8*, 630-632.
- (2) Park, J.; An, K.; Hwang, Y.; Park, J.-G.; Noh, H.-J.; Kim, J.-Y.; Park, J.-H.; Hwang, N.-M.; Hyeon, T. *Nature Materials* **2004**, *3*, 891.
- (3) Lattuada, M.; Hatton, T. A. *Langmuir* **2007**, *23*, 2158-2168.
- (4) Small, J. A.; Robert L. Watters, J., Report of investigation-Reference Material 8011 National Institute of Standards & Technology: Gaithersburg, 2015.
- (5) Meli, F.; Klein, T.; Buhr, E.; Frase, C. G.; Gleber, G.; Krumrey, M.; Duta, A.; Duta, S.; Korpelainen, V.; Bellotti, R.; Picotto, G. B.; Boyd, R. D.; Cuenat, A. *Measurement Science and Technology* **2012**, *23*.
- (6) Bienert, R.; Emmerling, F.; Thünemann, A. F. *Analytical and Bioanalytical Chemistry* **2009**, *395*, 1651.